Table 1. Gene expression profiles in WT and p53-KO mice. Mice were exposed to 300 ppm benzene for 6 hr/day, 5 days/week, for 2 weeks, and killed on day 12.[a]

Category	Gene name[b]	Fold change WT	Fold change KO	Accession number
Cell cycle	*Calcyclin*	1.08	1.89	X66449
	Cyclin B1	0.85	1.48	X64713
	Cyclin D3	0.83	1.20	M86186
	Cyclin G1	1.67	1.32	L49507
	Dmp1	2.01	2.81	U70017
	Gadd 45[c]	1.63	(—)	U00937
	JNK2	1.07	1.82	AB005664
	KSR1; protein kinase related to Raf protein kinase	1.11	2.57	U43585
	mLimk1; *Mus musculus* protein kinase	2.67	1.18	X86569
	Mph1/Rae 28; polycomb binding protein	4.97	0.06	U63386
	Nsg1; similar to mouse *p21*	2.45	1.83	AV347030
	p21[c]	1.37	(—)	U09507
	p53	1.03	0.13	U59758
	PERK	0.81	1.63	AF076681
	SNK; serum inducible kinase	1.68	1.02	M96163
	Tsc-2	2.00	1.25	U37775
	Wee-1[c]	1.95	(—)	D30743
	Wig-1; *p53*-inducible zinc finger protein	1.83	0.07	AF012923
Growth factor	*EGFB-3*; epidermal growth factor binding protein 3	1.92	0.69	M17962
	GPCR; *EB11*	0.01	0.97	L31580
	Growth hormone	0.99	1.73	X02891
	IGFBP-6 (s)	2.88	0.10	X81584
	PGRP; tumor necrosis factor super family 3-like	0.95	1.80	AF076482
	Placental growth factor	1.13	2.14	X80171
DNA damage /repair	*Rad50*	1.23	0.40	U66887
	Rad51	0.72	0.08	AV311591
Apoptosis	*Apaf-1*	1.16	1.75	AF064071
	Bax-alpha	1.20	1.21	L22472
	Bcl-2 alpha	0.91	1.66	L31532
	Caspase-9	0.83	1.59	AB019600
	Caspase-9S	0.84	2.26	AB019601
	Caspase-11	2.49	1.22	Y13089
	Caspase-12	0.86	0.18	Y13090
	ELK1; member of ETS oncogene family	1.33	2.06	X87257
	Metaxin2	0.95	1.55	AF053550
	p58; protein kinase inhibitor (*PKI*)	1.55	0.81	U28423
	Smad6	1.36	1.92	AF010133
	Siva (proapoptotic protein)	0.88	1.62	AF033115
	WISP1	0.68	1.26	AF100777
	WISP2	0.83	8.32	AF100778
Oxidative stress	*Aldehyde dehydrogease 4*	1.07	2.44	U14390
	Cox5b	1.07	1.56	X53157
	Cox7a-L	0.97	1.51	AF037371
	Cui/Zn-SOD	1.19	1.63	M35725
	Glyceraldehyde-3-phosphate dehydrogenase	1.06	3.34	M32599
	LDH1; lactate dehydrogenase 1	1.13	2.34	AW123952
	LDH2; lactate dehydrogenase 2	0.97	1.72	X51905
	Metallothionein 1	4.89	0.93	V00835
Metabolic enzyme	*CYP2E1*	2.13	1.72	X01026
	CYP7B1	1.84	1.11	U36993
	MPO; myeloperoxidase	1.68	1.49	X15378
Hemopoiesis	*ALK-1*; TGF-beta type 1 receptor	2.53	2.71	Z31664
	Beta-spectrin 3	1.78	0.87	AF026489
	CD3-theta T cell receptor	1.07	2.37	L03353
	Fra-2; *fos*-related antigen 2	1.78	1.78	X83971
	IL-4	0.91	1.95	M25892
	M-CSF; macrophage colony-stimulating factor	1.03	2.13	M21952
	Mac-1 alpha	0.74	1.93	X07640
	Mg11; IFN-induced	0.88	1.75	U15635
	MTCP-1; mature T cell proliferation 1	1.52	1.28	Z35294
	NFAT-1; nuclear factor of activated T cells 1	0.60	2.02	U36576
	Phospholipase A_2	1.35	1.77	U18119
	PI3K catalytic subunit p110 delta	2.36	0.18	U86587
	S100 calcium-binding protein A13	1.24	1.78	X99921
	STAT5B	0.91	1.74	AJ237939
	TCF; T-cell factor, alternatively spliced	1.00	2.11	AF107298
	TNFRrp; lymphotoxin-beta receptor	2.06	1.71	L38423
	Nr1il; vitamin D receptor	2.54	1.60	D31969
Oncogene	*Fes*	0.81	1.79	X12616
	c-*fos*	1.57	0.94	V00727
	RAB17; member of *RAS*.oncogene family	2.42	1.53	X70804
	Wnt-1/INT-1	1.72	1.23	M11943
Fatty acid β-oxidation	Acyl-CoA thioesterase	2.44	0.38	Y14004
	Adipose fatty acid binding protein	1.75	1.25	M20497

[a]The studies involved two to four animals; data were obtained from the use of the Affymetrix gene chips. Mice were killed on day 12, immediately after benzene exposure (see Figure 1, "Experimental Schedule"). [b]Information for GenBank (http://www.ncbi.nlm.nih.gov/Genbank/index.html). [c]No data available for p53-KO mice.

p53-KO mice, these genes did not change their expression level with benzene exposure. Table 3C shows that some changes in gene expression were undetectable because of the function of the *p53* gene, which can be "visualized" in the p53-KO microarray (Figure 4). Namely, data from toxicogenomics studies of specific gene KO mice could possibly disclose homeostatic balances undetectable in conventional WT mice.

Cell Cycle–Regulating Genes in p53-KO Mice and Wild-Type Mice

Cyclin genes were generally activated in p53-KO mice after benzene exposure, whereas cell cycle–regulating genes including the G2/M arrest-related gene *cyclin G1* (Kimura et al. 2001) were upregulated in WT mice. These findings indicate that the hemopoietic cell cycle is still functional in p53-KO mice during benzene exposure, whereas in WT mice it is arrested because of alterations in the expression of cell-cycle checkpoint genes, particularly the *p53* gene (Yoon et al. 2001b).

Some upstream genes encoding *p53*, such as *Dmp1* and *Raf-1* of the p53-KO mice, compared with those of the corresponding experimental groups of the WT mice, were upregulated to a similar extent or were more strongly enhanced in their expression. This is another indication of the role of the p53-mediated pathway in the mechanism of benzene toxicity associated with cell cycle regulation. Such information could be important in helping investigators to understand yet unknown mechanisms of chemical toxicity.

It is important to note that such a conclusion possibly can be drawn by carefully and simultaneously screening different expression patterns of many genes with interrelated functions, including genes showing small changes in expression levels (about 1.5- to 2-fold). The investigation of the expression levels of a limited number of genes generally may not provide insight into the main mechanism of chemical toxicity or clues to the particular role of each of the investigated genes in this mechanism. Toxicogenomics may have a strong advantage from this point of view (Inoue 2003).

Apoptosis-Related Genes in p53-KO Mice and Wild-Type Mice

The microarray analysis results of the p53-KO mice reminded us of the importance of the *p53* gene in the mechanism of benzene toxicity. The genes activated by the *p53* gene, including *p21*, *caspase 11* (Choi et al. 2001; Kang et al. 2000), and *cyclin G1* (Kimura et al. 2001), were distinctly upregulated in the benzene-exposed WT mice (Table 1). It is interesting that *caspase 11* instead of *caspase 9* was highly expressed after benzene exposure. This suggests that the p53-mediated activation of *caspase 11* is an important signaling pathway of apoptosis of bone marrow cells

Table 2. Expression profiles of the genes.

Category	Gene name[a]	Reference
Metabolic enzyme	*CYP2E1*	Zhang et al. 2002
	MPO	Schattenberg et al. 1994
Cell cycle	*p53*	Boley et al. 2002
	p21 (waf 1)	Boley et al. 2002
	Cyclin G	Boley et al. 2002
	Gadd 45	Boley et al. 2002
Apoptosis	*Bax*-alpha	Boley et al. 2002
Oncogene	c-*fos*	Ho and Witz 1997

[a]Information for GenBank (http://www.ncbi.nlm.nih.gov/Genbank/index.html).

Table 3. Differences in alteration of gene expression between WT and p53-KO mice after benzene exposure.

Expression category	Gene abbreviations[a]
A. p53-independent benzene-induced decrease or increase	
Decrease WT: decreased p53-KO: decreased	*CR6, EGFBP-1, GDIA, GDI-alpha, mGk-6, Glut-3, HDGF, PKD1, ZO-1*
Increase WT: increased p53-KO: increased	*ALK-1, Angrp, cardiac troponin T, Ctsg, CYP2E1, Dmp1, Fmo3, fra-2, GHR, Gpr50, Hox-1.7, KIK-I, MPO, NEFA protein, NrLi1, Nsg-1, PN-1, RAB17, Sim1, Sox10, Tip30, TNFRrp, WBP9*
B. p-53-dependent benzene-induced decrease or increase	
Decrease WT: decreased p53-KO: unchanged	*Adcy6, ApoE, AQ1,* B cell antigen receptor, *Cam III, CCR9, E2F1, FATP4, Fscn1, GPCR (EB11), Ig kappa light chain, IgA, IgH, mur42, Pdk1, PPT-B, Prkm1, TP, TRBF1*
Increase WT: increased p53-KO: unchanged	Adipose fatty acid binding protein, *Adh-3, caspase-11, cyclin G1, CYP7B1, EGFB-3, emp-1, FKBP23, c-fos, Hox-4.9, Int-1, Lfc, Krtl-12, mLimk1, MDC2, Mtcp1, Nr2b1, p58 (PKI), Pcnt, PFK, Pkacb, PGII, PTG, beta-spectrin, SPI-3, SNK, TSC-2*
C. p53-KO–related decrease or increase by benzene exposure but no changes in the WT mice	
Decrease WT: unchanged p53-KO: decreased	*CalDAG-GEFI, Cbfa2, Dctn1, Fr1, Grl-1, Ig/EBP, Klra3, Mek5,MEP,*
Increase WT: unchanged p53-KO: increased	*24p3, 4E-BP2, Abcg2, ACRP, activine, Ahd3, Alp, Anx3, AOE372, Apaf1, BAG-1, BAP, bcl-2, calcyclin, canexin, caspase 9, COX8H, caspase 9S, CCR1, CD3 theta, CD71, CD143, Cox5b, Cox7a1, Ctla-2a, Cu/Zn-SOD, cyclin B1, DCIR, Dnmt2, Dpagt2, E4BP4, EPO, FACS, Fes, elk1, G6PD, G6PD-2, Galbp, Gapdh, Gcdh, Gdi2,* growth hormone, *Gnb-1, Gng3lg, H-2T18, HES-1, IGF-1, IL1bc, IL-4, IL-9, JSR1, LDH-1, LDH-2, mLigl, Lipo 1, Lrf, Ly-3, Ly-40, Jam, JNK2, Kcc1, KSR1, M-CSF, Mac-1 alpha, Mch6, Mg11, MHR23A, MmCEN3, Mrad17, MRP14, Mtx2, NFATp, NL, Nmo1, OERK, PAFR, Pde8, PERK, PGRP, Pla2g2c, PLGF, Pop2, Prkm9, Prtn3, RBP-L, Rga, S100A13, Siva, Smad 6, SPRR2J, Stat4, Stat 5B, TCF4, TOM1, trypsin 2, Tst*

[a]Information for GenBank (http://www.ncbi.nlm.nih.gov/Genbank/index.html).

triggered by benzene exposure. This novel observation associated with the benzene toxicity mechanism together with the downmodulation of *caspase 12* was similarly addressed using WT and p53-KO mice in the study of the mechanism of chronic obstructive urinary disturbances (Choi et al. 2001). The decrease in the expression level of *caspase 12* in the p53-KO mice after benzene exposure seems to be in good agreement with the previous report on *caspase 12* regulation by p53 (Choi et al. 2001).

Genes associated with oxidative stress were both up- and downregulated in the p53-deficient mice, which may be an indication of benzene-induced oxidative stress (Yoon et al. 2001a; Table 1). It is not clear why oxidative stress–associated genes are activated in p53-KO mice and not in WT mice, but this might reflect the deregulation of the redox cycle due to the absence of the *p53* gene and the consecutive counteractivation of antioxidant enzymes (Chandel et al. 2000). Apoptotic protease-activating factor 1 (*Apaf-1*), metaxin, and *Siva* genes were also upregulated in the benzene-exposed p53-KO mice (Table 1). The expression of these genes may suggest proapoptotic conditions induced by benzene exposure of p53-KO mice. However, survival or anti-apoptosis genes such as *bcl-2*, *caspase 9S* (an endogenous dominant negative of *caspase 9*) (Seol and Billiar 1999), and *Smad6* (antagonist of tumor growth factor-β [TGF-β] signaling) (Imamura et al. 1997) are also activated in p53-KO mice. PERK (endoplasmic reticulum resident kinase) upregulation in p53-KO mice indicates the triggering of the unfolded protein-response signaling pathway, resulting in the loss of cyclin D1 (Brewer and Diehl 2000).

Expression of DNA Repair–Related Genes in *p53* Gene Network

Despite the possible damage to the DNA of the bone marrow cells of a p53-KO mouse, the DNA repair system is not likely to be functioning efficiently in the p53-KO mice, as DNA repair–related genes that were actively functioning in the benzene-exposed WT mice were not activated but rather suppressed in the p53-KO mice. In association with cell proliferation and apoptosis, high expression levels of the tuberous sclerosis gene (*Tsc-2*), a tumor suppressor gene encoding tuberin, and metallothionein 1 gene were noted in the WT mice (Table 1), raising the possibility that these genes are regulated by the *p53* gene. The association of metallothionein with p53 transcriptional activity has

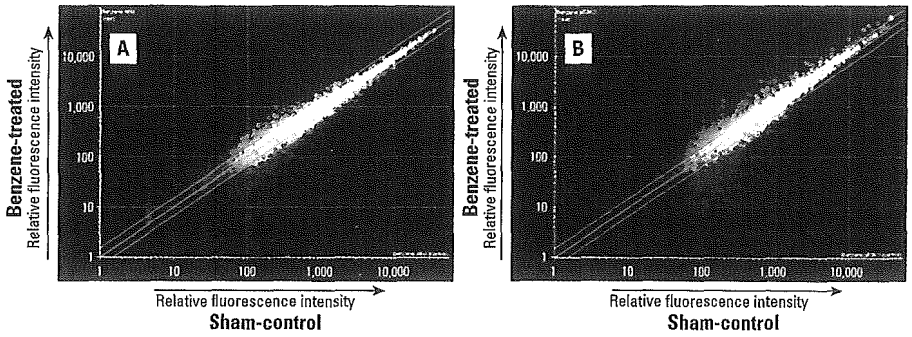

Figure 3. Scatterplots representing expression of genes in the bone marrow cells of benzene-exposed WT (*A*) and p53-KO mice (*B*) relative to expression of the genes in those of the corresponding sham-control mice, obtained using the Affymetrix system; *x*-axis and *y*-axis, respectively, indicate fluorescent signal intensity in the sham-control and benzene-exposed groups.

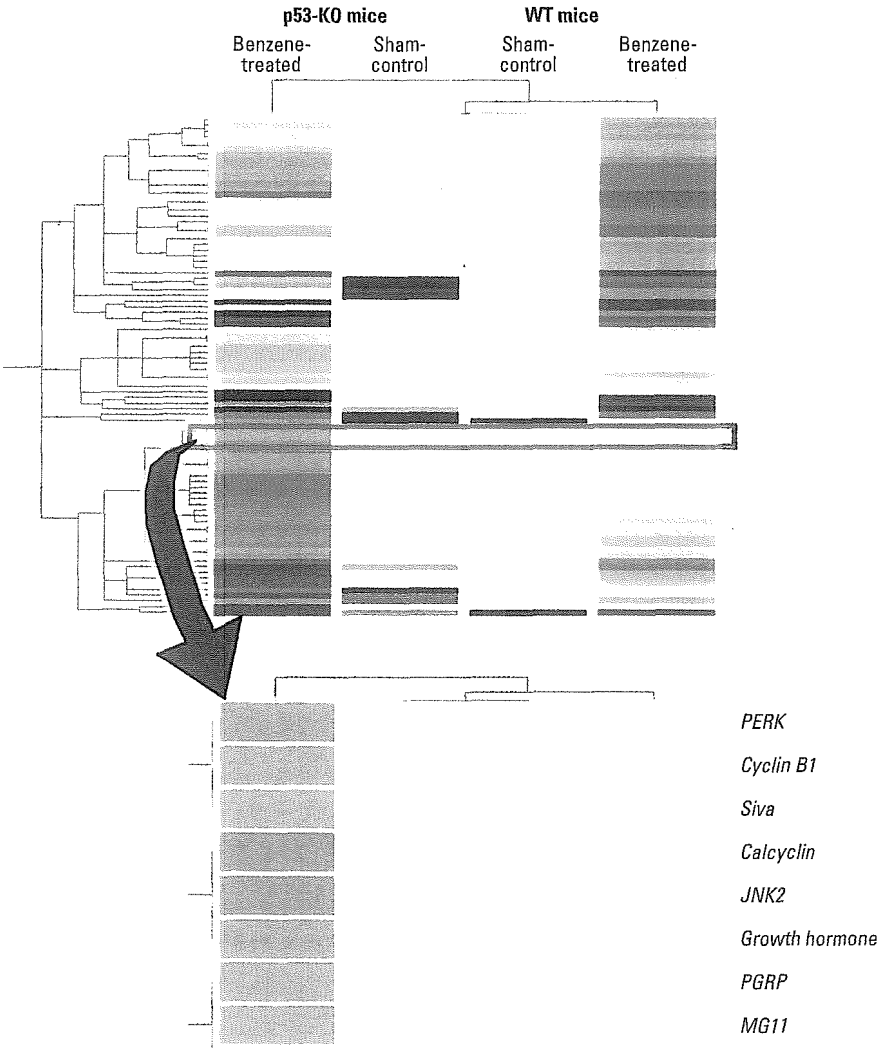

Figure 4. Clustering diagram of gene trees focused on particular genes of interest in the Affymetrix system. GeneSpring software was used to normalize the data. Clustering of microarray data revealed the standardized expression intensities of relevant genes shown by colors; from low expression level to high expression level, blue < yellow < orange < red. WT mice with or without benzene exposure, as well as p53-KO mice with or without benzene exposure are compared. A cluster of genes in the box (top) was found to consist of genes, the functions of which are related to cellular proliferation (bottom), and expressed only when p53 is knocked out, after benzene exposure. The average expression levels were obtained from two to four independent RNA samples from the mice. Genes in the box (top) are listed at the bottom; from the top: *PERK* (GenBank accession number AF076681), *cyclinB1* (GenBank accession number X64713), *Siva* (GenBank accession number AF033115), *calcyclin* (GenBank accession number X66449), *JNK2* (AB005664), growth hormone (GenBank accession number X02891), *PGRP* (GenBank accession number AF076482), *Mg11* (GenBank accession number U15635).

recently been postulated in an *in vitro* system in which metallothionein acts as a potent chelator to remove zinc from p53, thereby modulating p53 transcriptional activity (Meplan et al. 2000). The *Tsc-2* gene has recently been reported to regulate the insulin-signaling pathway mediated by protein kinase B (PKB/Akt) for cell growth (Gao and Pan 2001; Potter et al. 2002). It is noteworthy that *Tsc-2* is a target gene of 2,3,5-tris (glutathion-*S*-y) hydroquinone, a metabolite of hydroquinone for renal cell transformation (Lau et al. 2001). The high expression level of the *mph1/rae28* gene in the WT mice with severely suppressed bone marrow cellularity is noteworthy with respect to the maintenance of the activity of hemopoietic stem cells (Ohta et al. 2002). Furthermore, the Wnt-1 signaling pathway is also likely to be activated after benzene exposure, followed by the aberrant expressions of downstream genes such as *WISP1* and *WISP2* (Table 1). As the Wnt-1 signaling pathway was reported to regulate the proliferation and survival of various types of cell including B lymphocytes (Reya et al. 2000), the activation of both *mph1/rae28* and *Wnt-1* genes may be associated with the rapid recovery of suppressed bone marrow cellularity after cessation of benzene exposure.

Summary

As described above, the results of our cDNA microarray suggest that p53-KO mice are not resistant to benzene-induced toxic effects. These results were comparable with the dynamic protective responses of C57BL/6, WT mice at the gene functional level. On the basis of these observations, the effects of benzene on the bone marrow cells of p53-KO mice can be summarized as follows: *a*) cellular damage due to benzene metabolites and oxidative stress, *b*) dysfunction of the machinery of cell cycle arrest for repairing damaged DNA, resulting in continuous cycling of damaged cells even without undergoing repair, *c*) inhibition of apoptosis by both disruption of p53-dependent proapoptotic signaling and activation of survival genes, and *d*) failure of activating DNA repair genes. Such phenomena may lead to the increase in cell mutation frequencies at the candidate DNA locus, for instance, the *hprt* locus, responsible for benzene carcinogenesis, resulting in the development of hemopoietic malignancies. This hypothesis is based on multigene expression profiles that reasonably explain the high incidence and early onset of hemopoietic neoplasia, which were clearly observed in the p53 hetero- and homozygous KO mice chronically exposed to a critical dose of benzene for leukemogenicity tests (Kawasaki et al. Unpublished observation).

We also noted that the genes involved in fatty acid β oxidation such as the acyl-Co-A thioesterase gene and those encoding adipose fatty acid–binding proteins, which are commonly induced by peroxisome proliferators such as diethylhexylphthalate and clofibrate (Bartosiewicz et al. 2001), were also upregulated in the WT mice exposed to benzene (Table 1). A possible signaling pathway induced by benzene exposure is shown by a schematic in Figure 5. The present study using p53-KO mice elucidated the role of the *p53* gene not only in during benzene exposure, but also in the recovery state, and the gene expression profiling from p53-KO mice visualizes such oscillatory changes hidden behind the homeostatic balance organized by the *p53* gene in WT mice.

In conclusion, The cDNA microarray system used in this study revealed the mechanism of benzene toxicity by showing the altered expression of a number of benzene-affected genes including physiologic and toxicologic gene repertoires. Our data will provide valuable targets for the future investigation of the mechanism of benzene-induced toxicity and leukemogenicity.

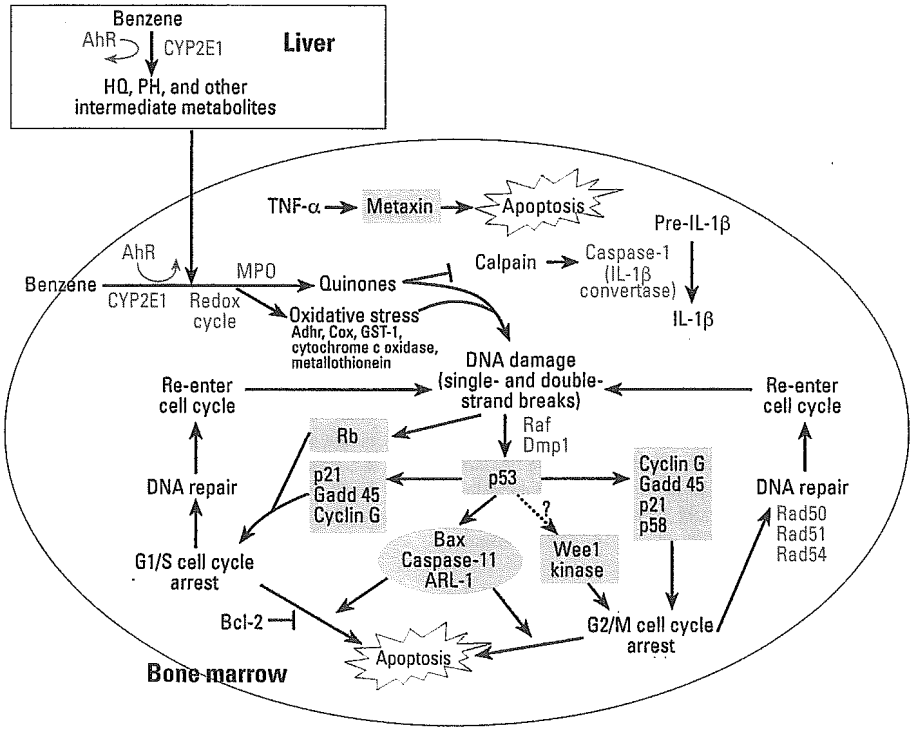

Figure 5. Mechanism of benzene toxicity at the molecular level based on the altered multigene expression profiles after benzene exposure. Benzene toxicity is dependent on AhR. CYP2E1 oxidizes benzene and produces quinones. Metabolites of benzene generated by cytochrome P450 monooxygenase and/or MPO trigger redox cycling consistent with the upregulation of genes for Adh4, Cox, glutathione *S*-transferase 1 (GST1) and metallothionein. Induction of p53 after DNA damage is the central toxicologic event, which readily induces the expression of p21, GADD45, and cyclin G, on one hand, the production of Bax, caspase 11, and ADP ribosylation factor–like protein 1 (ARL-1), and subsequently, the expression of Wee1 kinase. Induction of p21, in conjunction with Rb, results in the G1/S cell cycle arrest, whereas cyclin G and elongation factor 1 delta induces G2/M cell cycle arrest. Whether these cells in the cell cycle arrest further go into apoptosis or DNA repair depends on the participation of other cell signaling genes such as *bcl-2* and *Rad50*, *Rad51*, and *Rad54*. However, cells may mutate because of the possible failure of DNA repair.

References

Aksoy M, Erdem S, DinCol G. 1974. Leukemia in shoe-workers exposed chronically to benzene. Blood 44:837–841.

———. 1976. Types of leukemia in chronic benzene poisoning. A study in thirty-four patients. Acta Haematol 55:65–72.

Ambudkar SV, Gottesman MM, eds. ABC Transporters: Biochemical, Cellular, and Pharmacological Aspects. London:Academic Press, 1998.

Bartosiewicz MJ, Jenkins D, Penn S, Emery J, Buckpitt A. 2001. Unique gene expression patterns in liver and kidney associated with exposure to chemical toxicants. J Pharmacol Exp Ther 297:895–905.

Bernauer U, Vieth B, Ellrich R, Heinrich-Hirsch B, Janig GR, Gundert-Remy U. 1999. CYP2E1-dependent benzene toxicity: the role of extrahepatic benzene metabolism. Arch Toxicol 73:189–196.,
———. 2000. CYP2E1 expression in bone marrow and its intra- and interspecies variability: approaches for a more reliable extrapolation from one species to another in the risk assessment of chemicals. Arch Toxicol 73:618–624.
Boley SE, Wong VA, French JE, Recio L. 2002. p53 heterozygosity alters the mRNA expression of p53 target genes in the bone marrow in response to inhaled benzene. Toxicol Sci 66:209–215.
Brazma A, Hingamp P, Quackenbush J, Sherlock G, Spellman P, Stoeckert C, et al. 2001. Minimum information about a microarray experiment (MIAME)-toward standards for microarray data. Nat Genet 29:365–371.
Brewer JW, Diehl JA. 2000. PERK mediates cell-cycle exit during the mammalian unfolded protein response. Proc Natl Acad Sci USA 97:12625–12630.
Chandel NS, Vander Heiden MG, Thompson CB, Schumacker PT. 2000. Redox regulation of p53 during hypoxia. Oncogene 19:3840–3848.
Chen H, Eastmond DA. 1995. Synergistic increase in chromosomal breakage within the euchromatin induced by an interaction of the benzene metabolites phenol and hydroquinone in mice. Carcinogenesis 16:1963–1969.
Choi YJ, Mendoza L, Rha SJ, Sheikh-Hamad D, Baranowska-Daca E, Nguyen V, et al. 2001. Role of p53-dependent activation of caspases in chronic obstructive uropathy: evidence from p53 null mutant mice. J Am Soc Nephrol 12:983–992.
Cronkite EP, Bullis J, Inoue T, Drew RT. 1984. Benzene inhalation produces leukemia in mice. Toxicol Appl Pharmacol 75:358–361.
Cronkite EP, Drew RT, Inoue T, Hirabayashi Y, Bullis JE. 1989. Hematotoxicity and carcinogenicity of inhaled benzene. Environ Health Perspect 82:97–108.
Dean BJ. 1985. Recent findings on the genetic toxicology of benzene, toluene, xylenes and phenols. Mutat Res 154:153–181.
Eastmond DA, Smith MT, Irons RD. 1987. An interaction of benzene metabolites reproduces the myelotoxicity observed with benzene exposure. Toxicol Appl Pharmacol 91:85–95.
Farris GM, Robinson SN, Gaido KW, Wong BA, Wong VA, Hahn WP, et al. 1997. Benzene-induced hematotoxicity and bone marrow compensation in B6C3F1 mice. Fundam Appl Toxicol 36:119–129.
Gao X, Pan D. 2001. TSC1 and TSC2 tumor suppressors antagonize insulin signaling in cell growth. Genes Dev 15:1383–1392.
Gombart AF, Kwok SH, Anderson KL, Yamaguchi Y, Torbett BE, Koeffler HP. 2003. Regulation of neutrophil and eosinophil secondary granule gene expression by transcription factors C/EBP epsilon and PU.1. Blood 101:3265-3273.
Gut I, Nedelcheva V, Soucek P, Stopka P, Vodicka P, Gelboin HV, et al. 1996. The role of CYP2E1 and 2B1 in metabolic activation of benzene derivatives. Arch Toxicol 71:45–56.
Healy LN, Pluta LJ, James RA, Janszen DB, Torous D, French JE, et al. 2001. Induction and time-dependent accumulation of micronuclei in peripheral blood of transgenic p53+/– mice, Tg.AC (v-Ha-*ras*) and parental wild-type (C57BL/6 and FVB/N) mice exposed to benzene by inhalation. Mutagenesis 16:163–168.
Henderson RF. 1996. Species differences in the metabolism of benzene. Environ Health Perspect 104 (suppl 6):1173–1175.
Ho TY, Witz G. 1997. Increased gene expression in human promyeloid leukemia cells exposed to *trans,trans*-muconaldehyde, a hematotoxic benzene metabolite. Carcinogenesis 18:739–744.
Huff JE, Haseman JK, DeMarini DM, Eustis S, Maronpot RR, Peters AC, et al. 1989. Multiple-site carcinogenicity of benzene in Fischer 344 rats and B6C3F1 mice. Environ Health Perspect 82:125–163.
Imamura T, Takase M, Nishihara A, Oeda E, Hanai J, Kawabata M, et al. 1997. Smad6 inhibits signalling by the TGF-beta superfamily. Nature 389:622–626.
Inoue T. 2003. Introduction: Toxicogenomics—A New Paradigm of Toxicology. In: Toxicogenomics (Inoue T, Pennie WD, eds). Tokyo:Springer-Verlag, 3–11.
Jessen BA, Stevens GJ. 2002. Expression profiling during adipocyte differentiation of 3T3-L1 fibroblasts. Gene 299:95–100.
Kang SJ, Wang S, Hara H, Peterson EP, Namura S, Amin-Hanjani S, et al. 2000. Dual role of caspase-11 in mediating activation of caspase-1 and caspase-3 under pathological conditions. J Cell Biol 149: 613–622.
Kimura SH, Ikawa M, Ito A, Okabe M, Nojima H. 2001. Cyclin G1 is involved in G2/M arrest in response to DNA damage and in growth control after damage recovery. Oncogene 20:3290–3300
Kolachana P, Subrahmanyam VV, Meyer KB, Zhang L, Smith MT. 1993. Benzene and its phenolic metabolites produce oxidative DNA damage in HL60 cells *in vitro* and in the bone marrow *in vivo*. Cancer Res 53:1023–1026.
Laskin DL, Heck DE, Punjabi CJ, Laskin JD. 1996. Role of nitric oxide in hematosuppression and benzene-induced toxicity. Environ Health Perspect 104(suppl 6):1283–1287.
Lau SS, Monks TJ, Everitt JI, Kleymenova E, Walker CL. 2001. Carcinogenicity of a nephrotoxic metabolite of the "nongenotoxic" carcinogen hydroquinone. Chem Res Toxicol 14:25–33.
Lee EW, Garner CD. 1991. Effects of benzene on DNA strand breaks *in vivo* versus benzene metabolite-induced DNA strand breaks *in vitro* in mouse bone marrow cells. Toxicol Appl Pharmacol 108:497–508.
Low LK, Lambert C, Meeks J, Naro P, Mackerer CR. 1995. Tissue-specific metabolism of benzene in Zymbal gland and other solid tumor target tissues in rats. J Am Coll Toxicol 14:40–60.
Maltoni C, Ciliberti A, Cotti G, Conti B, Belpoggi F. 1989. Benzene, an experimental multipotential carcinogen: results of the long-term bioassays performed at the Bologna Institute of Oncology. Environ Health Perspect 82:109–124.
Meplan C, Richard MJ, Hainaut P. 2000. Metalloregulation of the tumor suppressor protein p53: zinc mediates the renaturation of p53 after exposure to metal chelators *in vitro* and in intact cells. Oncogene 19:5227–5236.
Moran JL, Siegel D, Sun XM, Ross D. 1996. Induction of apoptosis by benzene metabolites in HL60 and $CD34^+$ human bone marrow progenitor cells. Mol Pharmacol 50:610–615.
Niculescu R, Bradford HN, Colman RW, Kalf GF. 1995. Inhibition of the conversion of pre-interleukins-1 alpha and 1 beta to mature cytokines by *p*-benzoquinone, a metabolite of benzene. Chem Biol Interact 98:211–222.
Ohta H, Sawada A, Kim JY, Tokimasa S, Nishiguchi S, Humphries RK, et al. 2002. Polycomb group gene rae28 is required for sustaining activity of hematopoietic stem cells. J Exp Med 195:759–770.
Potter CJ, Pedraza LG, Xu T. 2002. Akt regulates growth by directly phosphorylating Tsc2. Nat Cell Biol 4:658–665.
Reya T, O'Riordan M, Okamura R, Devaney E, Willert K, Nusse R, et al. 2000. Wnt signaling regulates B lymphocyte proliferation through a LEF-1 dependent mechanism. Immunity 13:15–24.
Ross D. 2000. The role of metabolism and specific metabolites in benzene-induced toxicity: evidence and issues. J Toxicol Environ Health A 61:357–372.
Ross D, Siegel D, Schattenberg DG, Sun XM, Moran JL. 1996. Cell-specific activation and detoxification of benzene metabolites in mouse and human bone marrow: identification of target cells and a potential role for modulation of apoptosis in benzene toxicity. Environ Health Perspect 104(suppl 6):1177–1182.
Schattenberg DG, Stillman WS, Gruntmeir JJ, Helm KM, Irons RD, Ross D. 1994. Peroxidase activity in murine and human hematopoietic progenitor cells: potential relevance to benzene-induced toxicity. Mol Pharmacol 46:346–351.
Schlosser MJ, Shurina RD, Kalf GF. 1989. Metabolism of phenol and hydroquinone to reactive products by macrophage peroxidase or purified prostaglandin H synthase. Environ Health Perspect 82:229–237.
Schrenk D, Orzechowski A, Schwarz LR, Snyder R, Burchell B, Ingelman-Sundberg M, et al. 1996. Phase II metabolism of benzene. Environ Health Perspect 104(suppl 6):1183–1188.
Seol DW, Billiar TR. 1999. A caspase-9 variant missing the catalytic site is an endogenous inhibitor of apoptosis. J Biol Chem 274:2072–2076.
Smith MT, Yager JW, Steinmetz KL, Eastmond DA. 1989. Peroxidase-dependent metabolism of benzene's phenolic metabolites and its potential role in benzene toxicity and carcinogenicity. Environ Health Perspect 82:23–29.
Snyder CA, Goldstein BD, Sellakumar AR, Bromberg I, Laskin S, Albert RE. 1980. The inhalation toxicology of benzene: incidence of hematopoietic neoplasms and hematotoxicity in ARK/J and C57BL/6J mice. Toxicol Appl Pharmacol 54:323–331.
Snyder R, Hedli CC. 1996. An overview of benzene metabolism. Environ Health Perspect 104(suppl 6):1165–1171.
Snyder R, Kalf GF. 1994. A perspective on benzene leukemogenesis. Crit Rev Toxicol 24:177–209.
Subrahmanyam VV, Doane-Setzer P, Steinmetz KL, Ross D, Smith MT. 1990. Phenol-induced stimulation of hydroquinone bioactivation in mouse bone marrow *in vivo*: possible implications in benzene myelotoxicity. Toxicology 62:107–116.
Subrahmanyam VV, Ross D, Eastmond DA, Smith MT. 1991. Potential role of free radicals in benzene-induced myelotoxicity and leukemia. Free Radic Biol Med 11:495–515.
Tsukada T, Tomooka Y, Takai S, Ueda Y, Nishikawa S,

Yagi T, et al. 1993. Enhanced proliferative potential in culture of cells from p53-deficient mice. Oncogene 8:3313–3322.

Valentine JL, Lee SS, Seaton MJ, Asgharian B, Farris G, Corton JC, et al. 1996. Reduction of benzene metabolism and toxicity in mice that lack CYP2E1 expression. Toxicol Appl Pharmacol 141:205–213.

Vigliani EC, Forni A. 1976. Benzene and leukemia. Environ Res 11:122–127.

Ward IM, Minn K, van Deursen J, Chen J. 2003. p53 Binding protein 53BP1 is required for DNA damage responses and tumor suppression in mice. Mol Cell Biol 23:2556–2563.

Wolman SR. 1977. Cytologic and cytogenetic effects of benzene. J Toxicol Environ Health 2(suppl):63–68.

Yager JW, Eastmond DA, Robertson ML, Paradisin WM, Smith MT. 1990. Characterization of micronuclei induced in human lymphocytes by benzene metabolites. Cancer Res 50:393–399.

Yoon BI, Hirabayashi Y, Kaneko T, Kodama Y, Kanno J, Yodoi J, et al. 2001a. Transgene expression of thioredoxin (TRX/ADF) protects against 2,3,7,8-tetrachlorodibenzo-*p*-dioxin (TCDD)-induced hematotoxicity. Arch Environ Contam Toxicol 41:232–236.

Yoon BI, Hirabayashi Y, Kawasaki Y, Kodama Y, Kaneko T, Kanno J, et al. 2002. Aryl hydrocarbon receptor mediates benzene-induced hematotoxicity. Toxicol Sci 70:150–156.

Yoon BI, Hirabayashi Y, Kawasaki Y, Kodama Y, Kaneko T, Kim DY, et al. 2001b. Mechanism of action of benzene toxicity: cell cycle suppression in hemopoietic progenitor cells (CFU-GM). Exp Hematol 29:278–285.

Zhang S, Cawley GF, Eyer CS, Backes WL. 2002. Altered ethylbenzene-mediated hepatic CYP2E1 expression in growth hormone-deficient dwarf rats. Toxicol Appl Pharmacol 179:74–82.

ACADEMIC PRESS

Available online at www.sciencedirect.com
SCIENCE DIRECT®

Toxicology and Applied Pharmacology 190 (2003) 251–261

Toxicology and Applied Pharmacology

www.elsevier.com/locate/taap

Evaluation of nonthreshold leukemogenic response to methyl nitrosourea in p53-deficient C3H/He mice

Yoko Hirabayashi,[a,*] Kazuko Yoshida,[b] Shin-ichi Aizawa,[c] Yukio Kodama,[a] Jun Kanno,[a] Yuji Kurokawa,[a] Isao Yoshimura,[d] and Tohru Inoue[a]

[a] *Cellular and Molecular Toxicology Division, Center for Biological Safety and Research, National Institute of Health Sciences, Tokyo 158-8501, Japan*
[b] *Division of Biology and Oncology, National Institute of Radiological Science, Chiba 263-8555, Japan*
[c] *Laboratory for Vertebrate Body Plan, RIKEN Center for Developmental Biology, Kobe 650-0047, Japan*
[d] *Faculty of Engineering, Tokyo University of Science, Tokyo 162-8601, Japan*

Received 31 July 2002; accepted 2 April 2003

Abstract

The classic controversy of whether genotoxic chemicals induce cancers with or without a certain low-dose limit, i.e., the threshold, is revisited because of a number of current publications available addressing the plausibility of "practical" thresholds even for genotoxic carcinogens, the mechanism of which may be hypothesized to be due, in part, to a repair system composed of ordinarily available various defense mechanisms under the steady-state DNA damage. The question of whether an absolute nonthreshold or a relative nonthreshold, i.e., a "practical" threshold specifically in the low-dose level, is present may not be answered even with the use of a prohibitively large number of wild-type mice. Could the excessive incidence of tumorigenesis in p53-deficient mice contribute to our understanding of the threshold vs nonthreshold issue in genotoxic carcinogenesis? This is considered because an exaggeration of tumorigenesis in p53-deficient mice is hypothesized to reduce or eliminate the range of threshold due to the p53-deficiency-mediated reduction of DNA repair and apoptosis. The present study of chemical leukemogenesis in p53-deficient mice by transplantation assay was designed to answer this question. Briefly, 218 C3H/He mice were lethally irradiated and repopulated with bone marrow cells from wild-type, heterozygous p53-deficient, and homozygous p53-deficient C3H/He mice. This was followed by treatment with a single and graded dose of methyl nitrosourea at 6.6, 14.8, 33.3, 50.0, and 75.0 mg/kg body wt, with the vehicle-treated control groups treated with zero dose for each genotype. Whereas mice repopulated with p53-deficient bone marrow cells showed a marked reduction of the threshold for leukemogenicity, mice repopulated with wild-type bone marrow cells did not exhibit leukemia at a dose of 33.3 mg/kg body wt and showed a curve with a high probability for the linear regression model with a positive dose intercept, predicting a threshold by the likelihood ratio test. Thus, the failure of wild-type mice to show an increase in incidence of leukemogenesis at low doses of genotoxic carcinogens may be due not to a statistical rarity, but to various p53-related pharmacophysiological functions, possibly including DNA repair and apoptosis that may account for a threshold.

Keywords: Threshold and nonthreshold; Genotoxic carcinogenesis; p53 deficiency; p53 knockout mice; Chemical carcinogenesis

A threshold dose is the minimal dose that can elicit a response (Ehling et al., 1983). Nonthresholdedness is proposed solely based on the theoretical physical DNA hit that possibly induces one mutation in radiation carcinogenesis (Henschler, 1974; Muckerheide, 2001). Thus, the thresholds for carcinogenesis are believed to be infinite, which, like leprechauns, cannot be observed (Fry, 1989); whereas a statistically fairly clear threshold was reported for neoplasms in atomic bomb survivors (Pierce and Preston, 2000). Concerning chemical carcinogenesis, unlike radiation carcinogenesis (Henschler, 1974), nongenotoxic carcinogens that lack *Salmonella*-based mutagenicity are believed to induce thresholded carcinogenesis, involving an epigenetic event, as determined by the two-step assay for carci-

* Corresponding author. Cellular and Molecular Toxicology Division, Center for Biological Safety and Research, National Institute of Health Science, 1-18-1 Kamiyohga, Setagayaku, Tokyo 158-8501, Japan. Fax: +81-3-3700-9647.
E-mail address: yokohira@nihs.go.jp (Y. Hirabayashi).

0041-008X/03/$ – see front matter © 2003 Elsevier Science (USA). All rights reserved.
doi:10.1016/S0041-008X(03)00185-6

nogenesis (Berenblum and Shubik, 1947; Purchase, 1994). Recent accumulated data for chemical carcinogenesis further suggest the presence of thresholded carcinogenesis not only for nongenotoxic chemicals (Falk, 1976; Gehring and Blau, 1978; Zeise et al., 1987; Weisberger and Williams, 1989; Goodman and Counts, 1993; Counts and Goodman, 1995; Purchase and Auton, 1995), but also for genotoxic carcinogens (Williams et al., 2000). Various repair mechanisms for DNA damage and apoptosis as well as various oxidoreductase activities may account for the "practical threshold" (Hirabayashi et al., 1997; Moustacchi, 2000; O'Connor et al., 2000; Oesch et al., 2000; Schulte-Hermann et al., 2000; Seo et al., 2002).

Regardless of the number of mice used for bioassays, the regression line intersects the background baseline (United Nations Scientific Committee, 1986; Lovell, 2000; Chomentowski et al., 2000). This is true for both radiation and chemical carcinogeneses. Thus, experiments using a large number of mice have been unable to ascertain whether the genotoxic chemical process of carcinogenesis is due to threshold or nonthreshold carcinogenicity. Because a number of published studies of both p53-deficient mice (Harvey et al., 1993; Kemp et al., 1994; Kemp, 1995) and human patients with Li–Fraumeni syndrome (Li and Fraumeni, 1969; Malkin et al., 1990) have found a correlation between a high frequency of p53 deficiency and a high incidence of early-onset tumors, it is assumed that tumorigenesis can be induced at much lower doses of carcinogens in p53-deficient mice than in wild-type mice. If so, one can hypothesize that a dose of carcinogen that is not visibly carcinogenic in wild-type mice even when using a very large number may be carcinogenic in p53-deficient mice.

Accordingly, we attempted to test this hypothesis and to answer a related question: if p53-deficient mice do, in fact, manifest leukemogenicity at much lower doses than wild-type mice, would it be possible to detect such a nonthresholded leukemogenesis in p53-deficient mice even at doses lower than the no-effect dose level for wild-type mice? Furthermore, we utilized a bone marrow transplant (BMT)[1] assay (Hirabayashi et al., 1992; Yoshida et al., 2002) to focus on the carcinogenic action of methyl nitrosourea (MNU) in p53-deficient hemopoietic cells and thereby bypassing the effect of the dose–response relationship for MNU in nonhemopoietic tissues. Since hemopoietic neoplasms from transplants appear earlier than host diseases, competitive risks between hemopoietic neoplasms and other neoplasms from nonhemopoietic tissues can be also bypassed by the BMT assay.

In the present study, p53-deficient mice manifested a high correlation between the high incidence of early-onset leukemia and the decrease in the p53 gene dose. The likelihood ratio test (Dobson, 2002) was applied to evaluate the most fitting model for the experimental results from the wild-type as well as from the homozygous and heterozygous p53-deficient mice. Results are then discussed in the context of the threshold issue.

Materials and methods

Mice. Mice without the p53 gene, i.e., p53-knockout (KO) mice, were originally established by one of the authors (S.A.) (Tsukada et al., 1993), by gene targeting of embryonic stem cells from (DBA × C57BL/6) F_1, backcrossed with C57BL/6 mice. Hybrids with this heterozygous p53 deficiency were bred with normal C3H/HeNirsMs females. After 13 generations of backcrossing heterozygous p53-deficient mice with C3H/HeNirsMs, a homozygous p53-deficient C3H/HeNirsMs strain was obtained (Yoshida et al., 2002). In the present study, heterozygous p53-deficient (p53+/−) C3H/He mice were crossbred and we produced mice of each genotype as donors at the animal facility of the National Institute of Health Sciences (NIHS), Tokyo, Japan. Wild-type (p53+/+) C3H/He mice as recipients were obtained from Japan SLC (Hamamatsu, Japan). All the mice were housed under specific pathogen-free conditions, with a 12-h light–dark cycle at the animal facility of the NIHS. They were given acidified tap water and autoclaved food pellets ad libitum.

Preparation of bone marrow cells. After the animals were euthanized, a 27-gauge needle was inserted into the femoral bone cavity through the proximal and distal edges of the bone shafts, and the bone marrow (BM) cells were flushed out under pressure by injecting 2 ml of αMEM supplemented with a nucleotide mixture (Invitrogen Corp., Carlsbad, CA). A single-cell suspension was obtained by gently and repeatedly drawing the BM cells through the 27-gauge needle.

Irradiation. In the assay of hemopoietic progenitor cells (Till and McCulloch, 1961; Inoue et al., 1984), as well as in the repopulation assay for leukemogenesis (Hirabayashi et al., 1992; Yoshida et al., 2002), recipient mice were exposed to a lethal dose of radiation with 915 cGy delivered at a dose rate of 124 cGy/min with a ^{137}Cs-gamma irradiator (Gamma Cell 40; CSR, Toronto, Canada) using a 0.5-mm aluminum–copper filter.

Bone marrow transplantation. The BMT assay for a simplified leukemogenicity bioassay is described elsewhere (Hirabayashi et al., 1992; Yoshida et al., 2002). Briefly, BM cells (1×10^6) from 8-week-old heterozygous p53-deficient (p53+/−), homozygous p53-deficient (p53−/−), and wild-type (p53+/+) male mice were transplanted through the tail vein of 8-week-old, 915 cGy-irradiated, wild-type female recipients. In this procedure, the numbers of colony-forming cells from p53+/+, p53+/−, and p53−/− mice transferred

[1] Abbreviations used: BM, bone marrow; BMT, bone marrow transplantation; KO, knockout; MNU, *N*-methyl *N*-nitrosourea.

Table 1a
Histological disease spectra (Experiment 1)

Dose of MNU (mg/kg body wt)	Disease spectrum	Genotype of donors (*p53* gene)[a]		
		+/+	+/−	−/−
Vehicle	Neoplasms, hemopoietic	0.0 (0/11)	0.0 (0/10)	90.9 (10/11)
	Thymic lymphoma	0.0	0.0	72.7
	Nonthymic lymphoma	0.0	0.0	18.2
	Neoplasms, nonhemopoietic[b]	36.4 (4/11)	10.0 (1/10)	0.0 (0/11)
	Nonneoplastic lesions[c]	63.6 (7/11)	90.9 (9/10)	9.1 (1/11)
33.3	Neoplasms, hemopoietic	0.0 (0/10)	44.5 (4/9)	100.0 (10/10)
	Thymic lymphoma	0.0	22.2	90.0
	Nonthymic lymphoma	0.0	22.2	10.0
	Neoplasms, nonhemopoietic[b]	10.0 (1/10)	22.2 (2/9)	0.0 (0/10)
	Nonneoplastic lesions[c]	90.0 (9/10)	33.3 (3/9)	0.0 (0/10)
50.0	Neoplasms, hemopoietic	20.0 (2/10)	90.0 (9/10)	90.0 (9/10)
	Thymic lymphoma	10.0	80.0	50.0
	Nonthymic lymphoma	10.0	10.0	40.0
	Neoplasms, nonhemopoietic[b]	20.0 (2/10)	0.0 (0/10)	0.0 (0/10)
	Nonneoplastic lesions[c]	60.0 (6/10)	10.0 (1/10)	10.0 (1/10)
75.0	Neoplasms, hemopoietic	45.4 (5/11)	90.0 (9/10)	87.5 (7/8)
	Thymic lymphoma	27.3	70.0	25.0
	Nonthymic lymphoma	18.2	20.0	62.5
	Neoplasms, nonhemopoietic[b]	18.2 (2/11)	0.0 (0/10)	0.0 (0/10)
	Nonneoplastic lesions[c]	36.4 (4/11)	10.0 (1/10)	12.5 (1/8)

[a] Value in parentheses shows actual number of mice observed for each category per total number of mice of the group.
[b] Neoplasms, nonhemopoietic: pulmonary, hepatic, ovarian, and gastrointestinal tumors. As described in the text, these diseases are presumably recipient derived irrespective of the *p53* gene dose.
[c] Nonneoplastic lesions: cardioauricular thrombosis, renal sclerosis, and marrow failure. As described in text, these diseases are presumably recipient derived irrespective at the *p53* gene dose.

into each recipient mouse were 3.20, 3.08, and 2.60×10^2 progenitor cells, respectively. Only males were used as donors, and only females were used as recipients, in order to use the Y-chromosome-specific sequence as a marker that differentiates donor-derived neoplasms from recipient-derived neoplasms (Tanaka et al., 1991). In this transplantation assay, BM cells from p53-deficient or wild-type mice were equally effective in protecting against acute and subchronic radiation lethality, and the BM cellularity nearly attains equilibrium after 4 weeks of recuperation.

Methyl nitrosourea. At 4 weeks posttransplantation, 120 recipient mice (Experiment 1) and 98 mice (Experiment 2) were injected intraperitoneally with graded doses of MNU, ranging from 6.6 to 75.0 mg/kg body wt, or with vehicles for control, using 8 to 13 animals per dose (Tables 1a and b) (Terracini et al., 1976; Frei and Lawley, 1980; Inoue et al., 1984). Immediately before use, MNU (Nakarai-Tesque, Kyoto, Japan) was dissolved in a citrate buffer (0.01 M sodium citrate + 0.14 M NaCl, pH 5.5; Yamamoto et al., 1996) and injected intraperitoneally into recuperated mice. Two separate experiments, one for MNU doses 33.3, 50.0, and 75.0 mg/kg body wt, and the vehicle control (Table 1a) and the other for 6.6, 14.8, and 33.3 mg/kg body wt and the vehicle control (Table 1b) were performed. Recipients were assessed at least twice daily for behavioral parameters and were weighed weekly. All mice were monitored throughout their lifetime except for those showing symptoms of advanced leukemia such as anemia and palpable splenomegaly; these were euthanized at the agonal period and then examined hematopathologically. The other mice were also examined histopathologically.

Statistical analyses. Kaplan–Meier analyses with the Logrank test for data shown in Figs. 1 and 2 and the Mantel–Haenszel procedure for those shown in Fig. 3 (Microsoft Excel and its add-in software, "Statcel," OMS Ltd., Tokorozawa, Japan, 1998) were carried out to evaluate the significance of differences in data between vehicle controls and treated groups for mice of each genotype. Concerning the incidence of hemopoietic malignancies, the mice treated with an MNU dose of 6.6 mg/kg body wt and the vehicle-treated groups with p53−/− BM were evaluated by the *t* test, and the mean onset time of hemopoietic malignancies in each group shown in Fig. 4 was evaluated using Kaleida Graph version 3.501 computer software (Batschelet, 1979; Synergy Software, Reading, PA).

A likelihood ratio test was applied to evaluate the most fitting regression curve (Dobson, 2002). The likelihood for the "full model" and also for each regression curve, namely, a logistic, a linear, a quadratic, and a linear quadratic model, were calculated separately (Fig. 5A). The likelihood ratio test was also applied to the p53-deficient groups (Fig. 5B). Data were applied to the binomial distribution and a likelihood ratio test was carried to obtain $\pi(x_i)$ to maximize L (the likelihood) in the following equation:

$$L = \Pi_{i=1,yi}^{n} C_{ni}\pi(x_i)^{y_i}(1 - \pi(x_i))^{n_i - y_i}$$

Table 1b
Histological disease spectra (Experiment 2)

Dose of MNU (mg/kg body wt)	Disease spectrum	Genotype of donors (*p53* gene)[a]		
		+/+	+/−	−/−
Vehicle	Neoplasms, hemopoietic	N.D.	0.0 (0/11)	90.9 (10/11)
	Thymic lymphoma		0.0	54.5
	Nonthymic lymphoma		0.0	36.4
	Neoplasms, nonhemopoietic[b]	N.D.	18.2 (2/11)	0.0 (0/11)
	Nonneoplastic lesions[c]	N.D.	81.8 (9/11)	9.1 (1/11)
6.6	Neoplasms, hemopoietic	N.D.	7.7 (1/13)	92.3 (12/13)
	Thymic lymphoma		0.0	69.2
	Nonthymic lymphoma		7.7	23.1
	Neoplasms, nonhemopoietic[b]	N.D.	15.4 (2/13)	0.0 (0/13)
	Nonneoplastic lesions[c]	N.D.	76.9 (10/13)	7.7 (1/13)
14.8	Neoplasms, hemopoietic	N.D.	23.1 (3/13)	100.0 (13/13)
	Thymic lymphoma		7.7	84.6
	Nonthymic lymphoma		15.4	15.4
	Neoplasms, nonhemopoietic[b]	N.D.	15.4 (2/13)	0.0 (0/13)
	Nonneoplastic lesions[c]	N.D.	61.5 (8/13)	0.0 (0/13)
33.3	Neoplasms, hemopoietic	N.D.	50.0 (6/12)	100.0 (12/12)
	Thymic lymphoma		50.0	58.3
	Nonthymic lymphoma		0.0	41.7
	Neoplasms, nonhemopoietic[b]	N.D.	8.3 (1/12)	0.0 (0/12)
	Nonneoplastic lesions[c]	N.D.	41.7 (5/12)	0.0 (0/12)

[a] Value in parentheses shows actual number of mice observed for each category per total number of mice of the group. ND, not done.
[b] Neoplasms, nonhemopoietic: pulmonary, hepatic, ovarian, and gastrointestinal tumors. As described in the text, these diseases are presumably recipient derived irrespective of the *p53* gene dose.
[c] Nonneoplastic lesions: cardioauricular thrombosis, renal sclerosis, and marrow failure. As described in the text, these diseases are presumably recipent derived irrespective of the *p53* gene dose.

where, L is the likelihood; $\pi(x_i)$ is the ratio of cancer-bearing mice; x_i is the dose in group i; n_i is the number of animals; and y_i is the number of lymphomas/leukemias that developed per mouse.

In order to simplify the above equation, formulas such as $\pi(x_i) = \alpha + \beta x_i$ or $\pi(x_i) = \alpha + \beta x_i + \gamma x_i^2$ were substituted for the linear model or the quadratic model.

The "p" value, which is the ratio of both likelihood values calculated above, was obtained using the following equation (see Tables 3a and 3b):

$$p = L_1/L_2 \quad (0 < p \leq 1)$$

where, L_1 is a likelihood for the "full model," i.e., the alternative hypothesis and L_2 is a likelihood for a possible regression model, i.e., the null hypothesis.

In this equation, when the p value obtained from the likelihood ratio test is close to one, the regression line is assumed to be the most likely candidate. (Note, the maximum likelihood value is one.)

Results

Survival curves for the BMT assay

Fig. 1 shows survival curves for mice receiving a given dose of MNU. Survival of mice decreases with increasing dose of MNU; namely, the duration of survival was shorter for the p53−/− groups (Fig. 1, bottom) than for the p53+/+ groups (Fig. 1, top) at all MNU doses tested. For the p53−/− groups receiving MNU doses of 14.8 mg/kg body wt or higher, the duration of survival was 100 days or less. The durations of survival of the p53+/− groups (Fig. 1, middle) were intermediate between those of the p53−/− and the p53+/+ groups. As shown in Fig. 1, mice died of neoplasms other than nonhemopoietic malignancies or nonneoplastic diseases that are assumed to have originated from the recipient tissues.

Incidence of hemopoietic malignancies

The cumulative incidence of hemopoietic malignancies (i.e., malignant lymphomas/leukemias) developing in donor-cell-derived hemopoietic tissue is shown in Fig. 2. In groups repopulated with p53+/+ BM cells, hemopoietic malignancies developed only in one group of animals receiving an MNU dose 50.0 mg/kg body wt and in another group receiving 75.0 mg/kg body wt; the incidences of hemopoietic malignancies in these two groups were 20.0 and 45.0%, respectively. Kaplan–Meier analyses by the Logrank test (see Materials and methods) for each life span show significant differences between the 75.0-mg-treated and the vehicle-treated p53+/+ group ($p < 0.01$). All recipients of p53+/− BM cells who were treated with an MNU dose of 75.0 mg/kg body wt developed hemopoietic malignancies at an incidence of 90.0%, with onset and death

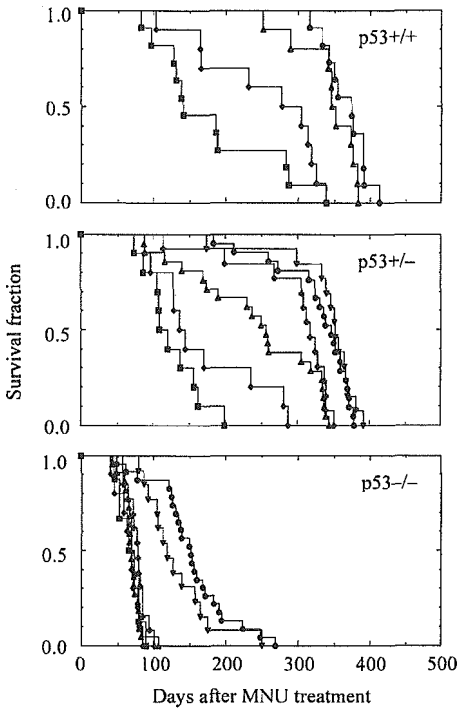

Fig. 1. Survival curves for the BMT assay (Hirabayashi et al., 1992; Yoshida et al., 2002). Recipients, lethally irradiated with 915 cGy, were repopulated with 1×10^6 BM cells from wild-type mice (p53+/+, top), from heterozygous p53-deficient mice (p53+/−, middle), and from homozygous p53-deficient mice (p53−/−, bottom); allowed to recuperate for 28 days before treatment of MNU; divided into six groups of 8 to 13 mice (Table 1a and b); and treated with a graded dose (mg/kg body wt) of MNU at 6.6 (reverse triangles), 14.8 (crosses), 33.3 (triangles), 50.0 (diamonds), or 75.0 (squares) or vehicle (circles) as a control. All the treated groups at more than 50.0 mg/kg body wt in the p53+/+ group, at more than 33.3 mg/kg body wt in the p53+/− groups, and more than 14.8 mg/kg body wt in the p53−/− groups showed a shorter life span than the respective vehicle control groups as determined by Kaplan–Meier analysis (Logrank test; $p < 0.01$). Two separate experiments were combined; the vehicle control and 33.3-mg-treated groups for p53+/− and p53−/− groups were repeated. No experiment was performed for doses lower than 33.3 mg/kg in the p53+/+ groups.

occurring earlier than in the p53+/+ group given the same dose of MNU (groups treated with more than 14.8 mg/kg body wt and the vehicle-treated groups repopulated with the p53+/− BM cells; $p < 0.01$, Fig. 2, middle). Although there was a high incidence of hemopoietic malignancies in the vehicle-treated p53−/− group, the life span of mice treated with more than 14.8 mg/kg body wt was statistically significantly shorter than that of mice treated with the vehicle ($p < 0.01$). In the bottom panel of Fig. 2, the incidence of lymphomas/leukemias corresponded to the survival curves shown in Fig. 1 (bottom).

Histological types of hemopoietic malignancies

Histological types of hemopoietic malignancies were induced in two separate experiments using different MNU doses; each of these experiments included the 33.3-mg-treated groups and the vehicle-treated groups. Results are tabulated separately in Tables 1a and 1b, and the combined incidences in each group are shown in Fig. 3. In the MNU-treated groups repopulated with BM cells from p53+/+, the incidences of thymic lymphomas and nonthymic lymphomas were observed to be 10.0% for both malignancies in the 50.0-mg-treated group, and 27.0 and 18.0%, respectively, in 75.0-mg-treated group. On the other hand, groups treated with 33.3 mg/kg body wt and vehicle showed no hemopoietic malignancies. As observed in Fig. 3, the p53+/− groups show higher incidences of hemopoietic malignancies as the MNU dose increases, in particular, the incidences of thymic lymphomas increase with the MNU dose; 7.7% for 14.8 mg/kg body wt treatment, 38.1% (average of two experiments) for 33.3 mg/kg body wt treatment, 80.0% for 50.0 mg/kg body wt treatment, and 70.0% for 75.0 mg/kg body wt treatment. On the other hand, the incidence of

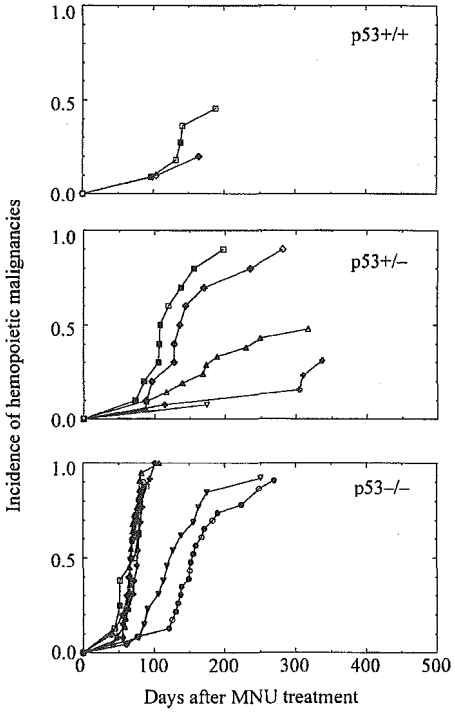

Fig. 2. Cumulative incidence of hemopoietic malignancies after MNU treatment in recipients that had been repopulated with BM cells from wild-type mice (p53+/+, top), from heterozygous p53-deficient mice (p53+/−, middle), and from homozygous p53-deficient mice (p53−/−, bottom). The MNU doses (mg/kg body wt) were 6.6 (reverse triangles), 14.8 (crosses), 33.3 (triangles), 50.0 (diamonds), and 75.0 (squares), and circles indicate control. In the p53+/+ groups (top), leukemias developed only in animals receiving MNU at a dose of 50.0 or 75.0 mg/kg body wt. Kaplan–Meier analyses for each life span show significant differences determined by the Logrank test between 75.0-mg treatment and vehicle treatment in the p53+/+ ($p < 0.01$) and between more than 14.8-mg treatment and vehicle treatment in the p53+/− and p53−/− groups ($p < 0.01$). Closed symbols, thymic lymphoma cases; open symbols, nonthymic lymphoma cases.

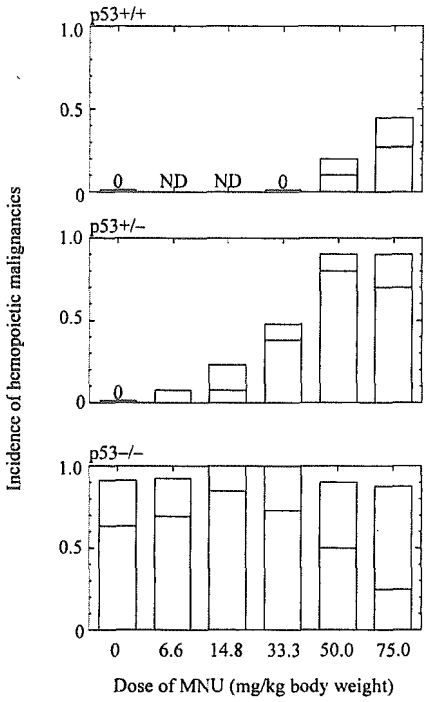

Fig. 3. Total incidence of hemopoietic malignancies induced by MNU in recipients that had been repopulated with BM cells from wild-type mice (p53+/+, top), heterozygous p53-deficient mice (p53+/−, middle), and homozygous p53-deficient mice (p53−/−, bottom panel). Hatched bar, thymic lymphoma incidence; open bar, nonthymic lymphoma incidence. The Mantel-Haenszel procedure shows significant relationship between MNU treatment and the occurrence of hemopoietic malignancy in the p53+/+ ($p = 0.00361$) and p53+/− groups ($p = 2.22 \times 10^{-16}$), but not in the p53−/− group ($p = 0.336$).

nonthymic lymphomas is lower and increases as the dose increases. In the p53−/− groups, the total incidences are all higher than 87.5%, including the vehicle-treated control

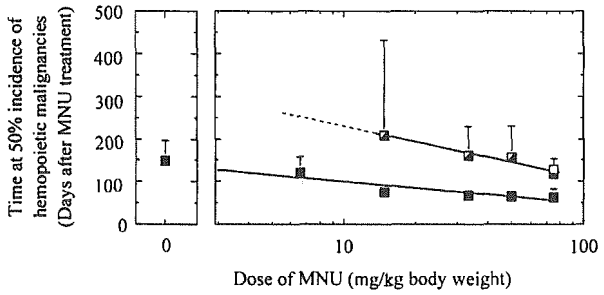

Fig. 4. The MNU dose is plotted on the abscissa against days to each 50% incidence of hemopoietic malignancies (see text). Data for mice repopulated with wild-type BM (p53+/+) cells are indicated by open squares; those with heterozygous p53-deficiency (p53+/−) by semiclosed squares; and those with homozygous p53deficiency (p53−/−) by closed squares. Vertical bars indicate SD of the means. Symbols without bars indicate smaller SDs than the size of symbols. Regression analysis shows significant differences in the two regression slopes between the p53+/− (−122.3 ± 18.01) and the p53−/− (−50.6 ± 15.55) groups ($p < 0.001$). (Heterozygous, $y = -122.3\ \mathrm{Log}(x) + 352.3$; homozygous, $y = -50.6\ \mathrm{Log}(x) + 149.9$).

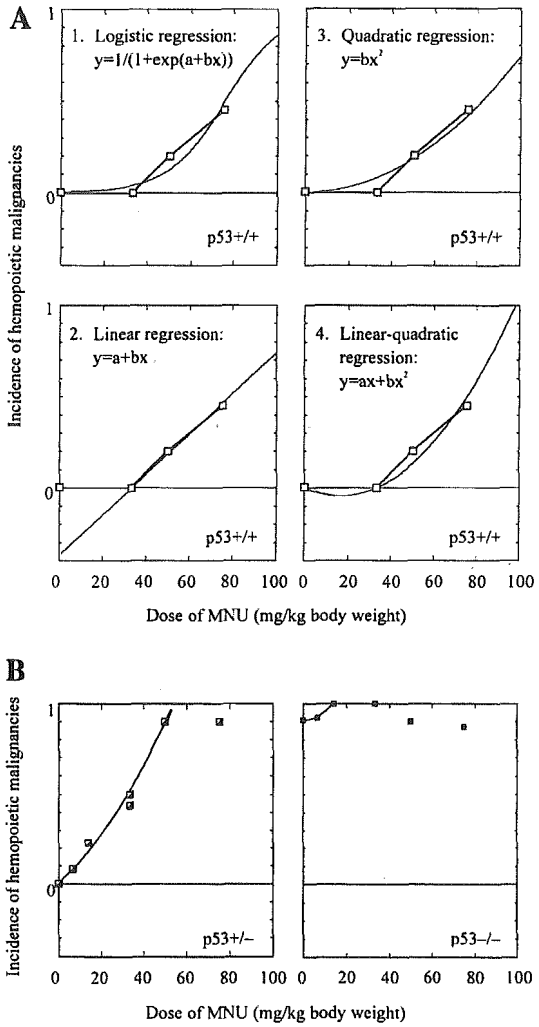

Fig. 5. (A) Incidence of hemopoietic malignancies in the p53+/+ groups is evaluated. Figures are replotted from Fig. 3. Curve fitting for logistic curve (A1), a linear model (hockey stick regression, A2), a quadratic model (A3), and a linear quadratic model (A4). See Discussion for details. Parameters for each formulation are tabulated in Table 3a. (B) Incidence of hemopoietic malignancies induced by MNU in heterozygous (p53+/−, left) and homozygous (p53−/−, right) p53-deficient groups. For the linear quadratic fittings, the lower part of data before neoplastic saturation was solely used, i.e., up to 50.0 mg/kg body wt for p53+/− groups and up to 14.8 mg/kg body wt for p53−/− groups. Parameters for each formulation are tabulated in Table 3b.

with an incidence of 90.9%. In particular, the incidences of thymic lymphomas show a distinct increase in groups treated with MNU up to 14.8 mg/kg body wt; i.e., vehicle control, 63.6%; 6.6 mg/kg body wt, 69.2%; and 14.8 mg/kg body wt, 84.6%. In contrast, the incidences of nonthymic lymphomas are lower than those of thymic lymphoma in dose groups higher than 33.3 mg/kg body wt; i.e., 33.3 mg/kg body wt, 27.3% (average of two experiments); 50.0 mg/kg body wt, 40.0%; and 75.0 mg/kg body wt, 62.5%.

As expected, all lymphomas/leukemias observed were found to be donor derived, associated with markers for the

Table 2
Risk indices for hemopoietic malignancies

p53 gene dose	Dose of MNU (mg/kg body wt)					
	0	6.6	14.8	33.0	50.0	75.0
p53+/+ (n = 2)	(−) (0.0/T[a])	N.D.	N.D.	(−) (0.0/T)[a]	(−) (20.0/T)[a]	0.353 (45.0/127.5)
p53+/− (n = 1)	(−) (0.0/T[a])	(−) (7.7/T[a])	0.113 (23.1/205.0)	0.298 (47.6/160.0)	0.581 (90.0/155.0)	0.763 (90.0/118.0)
p53−/− (n = 0)	0.602 (90.9/151.0)	0.763 (92.3/121.0)	1.342 (100.0/74.5)	1.481 (100.0/67.5)	1.387 (90.0/64.9)	1.382 (87.5/63.3)

Note. Risk indices (I) calculated using the equation; $I = Pi \times T^{-1}$ (see Results). Values in parentheses indicate Pi/T for each group. I = index of sensitivity to lymphomas/leukemias, Pi = lifetime incidence (percentage) of hemopoietic neoplasms (Tables 1a and b), and T = time (days) to reach median death (by probit) from hemopoietic neoplasms. ND, not done.

[a] T, no value because the case number of hemopoietic malignancies is 2 or less, median death time cannot be calculated.

homologous-recombination-specific sequence fused with the p53 and neo genes and for the Y-chromosome-specific sequence. All nonhemopoietic neoplasms such as pulmonary, hepatic, ovarian, and gastrointestinal tumors as well as nonneoplastic diseases, such as cardioauricular thrombosis and renal sclerosis, were demonstrated to be recipient-derived irrespective of the p53 gene dose (data not shown).

The vehicle-treated groups with homozygous p53 deficiency showed both thymic lymphomas and nonthymic lymphomas and the histological characteristics of these hemopoietic malignancies shown in Table 1a and 1b do not seem to be different from those induced by MNU and from those that developed spontaneously in the MNU-treated groups. However, the appearance of hemopoietic malignancies is clearly more rapid in the MNU-treated groups than that in vehicle-treated groups (Figs. 1 and 2); thus, statistical analyses were carried out separately afterward, but are presented all together in the figures.

Low-dose response in p53-deficient mice

In the p53+/+ and the p53+/− groups, the incidence of hemopoietic malignancies seemed to vary inversely with the animals' life spans (Figs. 1 and 2). Since the p53−/− groups manifested an almost 100.0% incidence of lymphomas/leukemias, their median life span was estimated by determining the 50.0% points on probit analyses. Fig. 4 shows the MNU dose plotted on the abscissa against the time to reach 50.0% of the population's death (median death) from lymphomas/leukemias. In Fig. 4, both the p53−/− and the p53+/− groups show longer median life spans with the decrease in the MNU dose (the dose response regression lines between the p53−/− and the p53+/− groups are p53−/−, $y = -50.6\ \mathrm{Log}(x) + 149.9$; p53+/−, $y = -122.3\ \mathrm{Log}(x) + 352.3$). Furthermore, the p53−/− groups were clearly sensitive as shown by the shorter and flatter curves for the median life spans. Since very few mice developed hemopoietic malignancies in the p53+/− group receiving MNU at 6.6 mg/kg body wt to yield significant data points (two leukemia cases), data from this group were not included but the missing values were extrapolated mathematically and shown as a broken line. Meaningful data were also not obtained from the p53+/+ groups receiving MNU less than 75.0 mg/kg body wt, because of a very low incidence of hemopoietic malignancies in the groups, and only a single data point is plotted as indicated by an open square at 75.0 mg/kg body wt.

Risk indices for hemopoietic malignancies

Since gene doses seemed to be a function of risk from neoplastic susceptibility, we calculated the risk index (I) from the data on the time (days) to median death from hemopoietic neoplasm obtained in Fig. 4:

$$I = P_i \times T^{-1}$$

where I is the index of sensitivity to lymphomas/leukemias, P_i is the lifetime incidence (percentage) of hemopoietic neoplasms (Table 1a and b), and T = time (days) to reach median death (by probit) from hemopoietic neoplasms.

The calculated risk indices (ordinate) are tabulated in Table 2. The risk index (I), reflecting the donor BM cells' sensitivity to MNU-induced lymphomagenesis/leukemogenesis, was found to be an inverse function of the p53 gene dose. In Table 2, risks for hemopoietic malignancies at the highest dose of MNU, 75.0 mg/kg body wt (rightmost column), are larger regardless of the p53 gene dose. In the column of 75.0-mg-treated groups, the p53−/− group is 1.8- and 3.9-fold larger than the p53+/− group and p53+/+ group, respectively. In the 14.8-mg-treated groups, the ratio between the risk in the p53+/− group and that in the p53−/− group is 11.9-fold, which is considerably larger than 1.8-fold in the 75.0-mg-treated groups; therefore, the p53−/− group is observed to be more sensitive than the p53+/− group and presumably also more than the p53+/+ group, when the MNU dose is low, when a lack of DNA repair may be most exaggerated.

Table 3a
Estimates of coefficient and the p value for each regression model in Fig. 6A

Regression	Formulation	Estimates of coefficient[a]		p value of likelihood ratio test[b]
		a	b	
Logistic	$y = 1/(1 + \exp(a + bx))$	5.73	7.55×10^{-2}	0.508
Linear	$y = a + bx$	-3.70×10^{-1}	1.11×10^{-2}	0.896
Quadratic	$y = bx^2$	—	7.41×10^{-5}	0.408
Linear quadratic	$y = ax + bx^2$	-5.23×10^{-3}	1.57×10^{-4}	0.513

[a] Estimates of coefficient listed here are maximized likelihood of each regression model obtained by calculation to approximate one by one.
[b] See Materials and methods for details.

Curve fitting for hemopoietic malignancies

The incidence of lymphomas/leukemias in each gene–dose group plotted against the MNU dose in Fig. 3 is replotted and shown in Fig. 5A and B. The p values obtained from the likelihood-ratio test were obtained by comparison between the "full model" and each regression model (see Materials and methods). For the p53+/+ groups, four possible regression curves for the MNU-induced leukemias were tested, i.e., a fitting to a logistic curve (Fig. 5A1), a linear model (hockey stick regression) (Fig. 5A2), a single quadratic model (Fig. 5A3), and a linear quadratic model (Fig. 5A4). Estimates of coefficients for each regression model are shown in Table 3a. The p values for each regression model against the full model are calculated and also shown in Table 3a. It is clear that, the highest p value is for the linear regression, i.e., 0.896, hence, implying that the linear regression has the highest possibility to fit the full model among the regression models. The p values indicate that this model is approximately twice as likely to fit as any of the other models. This result strongly suggests that the curve for the wild type is thresholded.

The curves for the p53-deficient groups were then evaluated whether they are nonthresholded or thresholded (Fig. 5B). Estimates of coefficients for a linear quadratic model are shown in Table 3b. The linear quadratic model for the p53−/− groups is the same as the full model since the linear quadratic model was estimated from only three observation points. The curves fit the linear quadratic model quite well, with p values that were relatively close to one. It can be concluded that the curves may be nonthresholded (p values of the likelihood ratio test: 0.88 and 1.00 for p53+/− and p53−/−, respectively).

Discussion

The dose–response relationship of genotoxic carcinogenicity has long been assumed to be nonthresholded (Henschler, 1974; Littlefield et al., 1980). Possible controversial evidence currently reported suggests, however, a nonthresholdness with "practical" threshold responses (Hirabayashi et al., 1997; Moustacchi, 2000; O'Connor et al., 2000; Oesch et al., 2000; Schulte-Hermann et al., 2000; Seo et al., 2002) or even a possible absolute thresholded response (Elhajouji et al., 1995; Kirsch-Volders et al., 2000; Williams et al., 2000). In the present study, an experimental trial was carried out to investigate whether genotoxicity-sensitive p53-deficient mice may provide useful evidence to help resolve the controversy of such threshold–nonthreshold issues in carcinogenicity testing by the BMT assay.

The carcinogenic threshold doses, below which carcinogenesis is not observed, have been recognized specifically in carcinogens that lack the *Salmonella*-based mutagenicity, such as the threshold determined for the detoxification by xenobiotic enzymes (Marcus and Rispin, 1988; Povey, 2000; Weisberger and Williams, 1989), for the modulation of cellular signal transduction (Purchase and Auton, 1995; Gehring and Blau, 1978), or for the various pharmacokinetical modulations of permeation and/or absorption through the cytoplasmic membrane (Falk, 1976; Gehring and Blau, 1978; Zeise et al., 1987). Recently, practical

Table 3b
Estimates of coefficient and the p value for regression to linear quadratic model in Fig. 6B

p53 deficiency	Estimates of coefficient[a]			p value of likelihood ratio test[b]
	a	b	c	
Heterozygous (p53+/−)	0.00	1.08×10^{-2}	1.40×10^{-4}	0.88
Homozygous (p53−/−)	9.09×10^{-1}	1.78×10^{-3}	5.92×10^{-4}	1.00[c]

[a] Estimates of coefficient listed here are maximized likelihood of linear quadratic model (formulation: $y = a + bx + cx^2$) obtained by calculation to approximate one by one.
[b] See Materials and methods for details.
[c] The linear quadratic model is the same as the full model since the linear quadratic model was estimated from only three observed points.

thresholds even for genotoxic carcinogens (Schulte-Hermann et al., 2000) have been proposed based on various anticarcinogenic defense mechanisms, such as an adaptative enhancement of excision repair mechanisms for DNA damage (Le et al., 1998; O'Connor et al., 2000; Smith and Seo, 2002), as well as based on detoxification, for example, by oxidoreductases for various DNA-damaging adducts formed such as epoxides (Bridges and Stamper, 1975; Oesch et al., 2000; Povey, 2000; Williams et al., 2000). On the other hand, there are reports disagreeing with those practical thresholds, indicating the sublinearity of DNA damage after inhibition of DNA ligase due to arsenic toxicity (Rudel et al., 1996) and the nonthresholded carcinogenicity observed for the toxicity due to 2-acetyl aminofluorene (Littlefield et al., 1980). Moreover, others describe the difficulty in distinguishing a thresholded carcinogenesis from a nonthresholded carcinogenesis (Terraccini et al., 1976).

Mice deficient in the p53 gene are known to be extremely susceptible to radiation as well as chemical carcinogens (Harvey et al., 1993; Kemp et al., 1994; Kemp, 1995: Yoshida et al., 2002), similar to the human counterpart, Li–Fraumeni syndrome (Li and Fraumeni, 1969; Malkin et al., 1990; Bougeard et al., 2003). In our study, MNU-treated mice repopulated with p53-deficient BM cells manifested an earlier onset and higher incidence of lymphomas/leukemias than those repopulated with p53+/+ BM cells (Figs. 1 and 2). The mechanisms underlying these early onset and high incidence responses are not fully determined as yet (Liao et al., 1998). However, hemopoietic neoplasms may have developed due to possible genomic instabilities related to the p53 gene deficiency, and the incidences are clearly higher than those in the vehicle-treated groups (French et al., 2001, Toft et al., 2002).

In the present study, the p53-deficient mice, both heterozygous and homozygous, showed an earlier onset and in some comparisons a higher incidence of lymphomas/leukemias induced by graded doses of MNU (Figs. 1 and 2). As shown in Fig. 2, the incidences of lymphomas/leukemias increased with the MNU dose. The overall incidence was greater in the p53-deficient groups than in the p53+/+ groups, whereas lymphomas/leukemias were observed only at MNU doses greater than 50.0 mg/kg body wt in the p53+/+ groups. In p53−/− groups, lymphomas/leukemias were observed even in those without MNU treatment. The precise mechanism of induction of such spontaneous tumors in the p53−/− mice is now the focus of much interest (Liao et al., 1998).

In both the p53−/− and p53+/− groups, life spans of all the treated groups, except the 6.6-mg-treated groups, were statistically significantly shorter than that of the vehicle-treated groups for each p53 gene dose (Fig. 2). Even the p53−/− group treated at a dose of 6.6 mg/kg body wt showed a significantly shorter life span than the vehicle-treated group when significances were evaluated by the *t* test based on the normal distribution and a significantly longer life span than those of groups treated with more than 14.8 mg/kg body wt when significances were evaluated by the Logrank test based on the Kaplan–Meier fitting.

In order to clarify the sensitivity of p53-deficient mice, the incidences of hemopoietic malignancies were plotted against the graded doses of MNU (Fig. 4). The slope for the p53−/− groups was 2.42-fold lower than that for the p53+/− groups ($p < 0.001$). Furthermore, treatment at 6.6 mg/kg body wt had limited effects on the p53+/− groups, with an incidence of lymphomas/leukemias of only 1 of 13 mice. The only effect in the p53+/+ groups was a small number of lymphomas/leukemias in those receiving 75.0 mg/kg body wt. This is close to the reported value of 1 of 40 mice (2.5%) at 25.0 mg of MNU/kg body wt (Terracini et al., 1976).

An analysis for the likelihood ratio test in the p53−/− and the p53+/− groups and the p53+/+ group showed that the full models for the former fit to the linear quadratic model ($p = 1.000$ and 0.88, respectively), i.e., nonthresholded, whereas the full model for the latter fits best a linear regression ($p = 0.896$), i.e., thresholded, although nonthresholdedness cannot be statistically rejected at present.

The C3H/He strain bred at the authors' laboratory was used in the present study. The C3H/He strain is known to have an incidence of 1.0% or less for myeloid leukemias as spontaneous hemopoietic malignancies without induction with carcinogenic chemicals or radiation exposure (Yoshida et al., 1997, 1986), which may have contributed to obtaining a statistically clear contrast in neoplastic incidence between treated groups and the control in the present study.

The present study is distinct because it shows usefulness of the p53−/− mice for quantitative carcinogenicity bioassays. The p53−/− mice were believed to have a high incidence of spontaneous tumors with an earlier onset similar to the induced tumors, and these spontaneous tumors are readily indistinguishable from induced tumors. Thus, they were considered not useful in carcinogenicity bioassay testing. However, as shown in the present study, as well as in the conventional whole-body assay, as long as only the C3H/He strain is used, the homozygous p53 deficiency has great advantages not only for induced tumorigenic sensitivity compared with the wild-type mice, especially in the low-dose level, but also for distinguishing induced tumors from spontaneous tumors within 100 days and for defining pure genotoxic carcinogenic agents.

The above findings suggest the failure to repair possible DNA damage due to the possible spontaneous p53 deficiency as in Li–Fraumeni syndrome (Bougeard et al., 2003) and/or known altered p53 functions during the course of senescence (Moragoda et al., 2002).

Acknowledgments

The authors thank Ms. M. Hojo, Ms. N. Katsu, and Ms. C. Kimura for help in manuscript preparation; Ms. E. Tachi-

hara, Ms. Y. Usami, and Ms. Y. Shinzawa for help with experiments; and Lillian Delmont and the late Eugene P. Cronkite for their constructive peer reviews and comments. Moreover, we thank Dr. Lucy M. Anderson for constructive editorial advices and suggestions specifically provided during the review of this manuscript are greatly appreciated. This research was supported by a grant for carcinogenic bioassay using biotechnology-derived recombinant mice (MHLW-Cancer Research-S8-2 and S11-5).

References

Batschelet, E., 1979. Introduction to Mathematics for Life Scientists. Springer-Verlag, Berlin.

Berenblum, I., Shubik, P., 1947. A new quantitative approach to the study of stages of chemical carcinogenesis in the mouse's skin. Br. J. Cancer 1, 383.

Bougeard, G., Brugieres, L., Chompret, A., Gesta, P., Charbonnier, F., Valent, A., Martin, C., Raux, G., Feunteun, J., Paillerets, B.B., Frebourg, T., 2003. Screening for TP53 rearrangements in families with the Li–Fraumeni syndrome reveals a complete deletion of the TP53 gene. Oncogene 22, 840–846.

Bridges, B.A., Stamper, J.G., 1975. Hypothetical dose–response curves for chronic exposures to mutagens or carcinogens subject to simple enzymatic detoxification in the mammalian body. Mutat. Res. 33, 87–91.

Chomentowski, M., Kellerer, A.M., Pierce, D.A., 2000. Radiation dose dependences in the atomic bomb survivor cancer mortality data: a model-free visualization. Radiat. Res. 153, 289–294.

Counts, J.L., Goodman, J.I., 1995. Hypomethylation of DNA: a possible epigenetic mechanism involved in tumor promotion. Prog. Clin. Biol. Res. 391, 81–101.

Dobson, A.J. (Ed.), 2002. An Introduction to Generalized Linear Models, second ed. Chapman & Hall/CRC, Washington, DC.

Ehling, U.H., Averbeck, D., Cerutti, P.A., Friedman, J., Greim, H., Kolbye Jr., A.C., Mendelsohn, M.L., 1983. International Commission for Protection against Environmental Mutagens and Carcinogens. ICPEMC publication no. 10, Review of the evidence for the presence or absence of thresholds in the induction of genetic effects by genotoxic chemicals. Mutat. Res. 123, 281–341.

Elhajouji, A., Van Hummelen, P., Kirsch-Volders, M., 1995. Indications for a threshold of chemically-induced aneuploidy in vitro in human lymphocytes. Environ. Mol. Mutagen. 26, 292–304.

Falk, H.L., 1976. Possible mechanisms of combination effects in chemical carcinogenesis. Oncology 33, 77–85.

Frei, J.V., Lawley, P.D., 1980. Thymomas induced by simple alkylating agents in C57BL/Cbi mice: kinetics of the dose response. J. Natl. Cancer Inst. 64, 845–856.

French, J.E., Lacks, G.D., Trempus, C., Dunnick, J.K., Foley, J., Mahler, J., Tice, R.R., Tennant, R.W., 2001. Loss of heterozygosity frequency at the Trp53 locus in p53-deficient (+/−) mouse tumors is carcinogen- and tissue-dependent. Carcinogenesis 22, 99–106.

Fry, R.J., 1989. The question of thresholds for carcinogenesis. Cancer Invest. 7, 299–300.

Gehring, P.J., Blau, G.E., 1978. Mechanisms of carcinogenesis: dose response. J. Environ. Pathol. Toxicol. 1, 163–179.

Goodman, J.I., Counts, J.L., 1993. Hypomethylation of DNA: a possible nongenotoxic mechanism underlying the role of cell proliferation in carcinogenesis. Environ. Health Perspect. 101 (Suppl. 5), 169–172.

Harvey, M., McArthur, M.J., Montgomery Jr., C.A., Butel, J.S., Bradley, A., Donehower, L.A., 1993. Spontaneous and carcinogen-induced tumorigenesis in p53-deficient mice. Nat. Genet. 5, 225–229.

Henschler, D., 1974. New approaches to a definition of threshold values for "irreversible" toxic effects? Arch. Toxicol. 32, 63–67.

Hirabayashi, Y., Inoue, T., Suda, Y., Aizawa, S., Ikawa, Y., Kanisawa, M., 1992. Hemopoietic neoplasms in lethally irradiated mice repopulated with bone marrow cells carrying the human c-myc oncogene: a repopulation assay. Exp. Hematol. 20, 167–172.

Hirabayashi, Y., Matsuda, M., Matumura, T., Mitsui, H., Sasaki, H., Tukada, T., Aizawa, S., Yoshida, K., Inoue, T., 1997. The p53-deficient hemopoietic stem cells: their resistance to radiation apoptosis, but lasted transiently. Leukemia 11 (Suppl. 3), 489–492.

Inoue, T., Cronkite, E.P., Commerford, S.L., Carsten, A.L., 1984. Residual toxicity in hematopoietic cells following a single dose of methylnitrosourea. Leuk. Res. 8, 105–116.

Kemp, C.J., 1995. Hepatocarcinogenesis in p53-deficient mice. Mol. Carcinog. 12, 132–136.

Kemp, C.J., Wheldon, T., Balmain, A., 1994. p53-deficient mice are extremely susceptible to radiation-induced tumorigenesis. Nat. Genet. 8, 66–69.

Kirsch-Volders, M., Aardema, M., Elhajouji, A., 2000. Concepts of threshold in mutagenesis and carcinogenesis. Mutat. Res. 464, 3–11.

Le, X.C., Xing, J.Z., Lee, J., Leadon, S.A., Weinfeld, M., 1998. Inducible repair of thymine glycol detected by an ultrasensitive assay for DNA damage. Science 280, 1066–1069.

Li, F.P., Fraumeni, J.F., 1969. Soft-tissue sarcomas, breast cancer, and other neoplasms: a familial syndrome? Ann. Intern. Med. 71, 747–752.

Liao, M.J., Zhang, X.X., Hill, R., Gao, J., Qumsiyeh, M.B., Nichols, W., Van Dyke, T., 1998. No requirement for V(D)J recombination in p53-deficient thymic lymphoma. Mol. Cell. Biol. 18, 3495–3501.

Littlefield, N.A., Farmer, J.H., Gaylor, D.W., Sheldon, W.G., 1980. Effects of dose and time in a long-term, low-dose carcinogenic study. J. Environ. Pathol. Toxicol. 3, 17–34.

Lovell, D.P., 2000. Dose–response and threshold-mediated mechanisms in mutagenesis: statistical models and study design. Mutat. Res. 464, 87–95.

Marcus, W.L., Rispin, A.S., 1988. Threshold carcinogenicity using arsenic as an example, in: Cothern, C., Mehlman, M., Marcus, W.L. (Eds.), Risk Assessment and Risk Management of Industrial and Environmental Chemicals, Vol. 15, Princeton Scientific Publishing, Princeton, NJ, pp. 133–159.

Malkin, D., Li, F.P., Strong, L.C., Fraumeni, J.F., Nelson, C.E., Kim, D.H., Kassel, J., Gryka, M.A., Bischoff, F.Z., Tainsky, M.A., Friend, S.H., 1990. Germ line p53 mutations in a familial syndrome of breast cancer, sarcomas, and other neoplasms. Science 250, 1233–1238.

Moragoda, L., Jaszewski, R., Kulkarni, P., Majumdar, A.P., 2002. Age-associated loss of heterozygosity of tumor suppressor genes in the gastric mucosa of humans. Am J. Physiol. Gastrointest. Liver Physiol. 282, G932–G936.

Moustacchi, E., 2000. DNA damage and repair: consequences on dose–responses. Mutat. Res. 464, 35–40.

Muckerheide J. (Ed.), 2001 Low-level radiation health effects: compiling the data, second edition, revision 4. Radiation, Science, & Health, (http://cnts.wpi.edu/RSH/Data_Docs/index.html).

O'Connor, P.J., Manning, F.C., Gordon, A.T., Billett, M.A., Cooper, D.P., Elder, R.H., Margison, G.P., 2000. DNA repair: kinetics and thresholds. Toxicol. Pathol. 28, 375–381.

Oesch, F., Herrero, M.E., Hengstler, J.G., Lohmann, M., Arand, M., 2000. Metabolic detoxification: implications for thresholds. Toxicol. Pathol. 28, 382–387.

Pierce, D.A., Preston, D.L., 2000. Radiation-related cancer risks at low doses among atomic bomb survivors. Radiat. Res. 154, 178–186.

Povey, A.C., 2000. DNA adducts: endogenous and induced. Toxicol. Pathol. 28, 405–414.

Purchase, I.F., 1994. Current knowledge of mechanisms of carcinogenicity: genotoxins versus non-genotoxins. Hum. Exp. Toxicol. 13, 17–28.

Purchase, I.F., Auton, T.R., 1995. Thresholds in chemical carcinogenesis. Regul. Toxicol. Pharmacol. 22, 199–205.

Rudel, R., Slayton, T.M., Beck, B.D., 1996. Implications of arsenic genotoxicity for dose response of carcinogenic effects. Regul. Toxicol. Pharmacol. 23, 87–105.

Schulte-Hermann, R., Grasl-Kraupp, B., Bursch, W., 2000. Dose–response and threshold effects in cytotoxicity and apoptosis. Mutat. Res. 464, 13–18.

Seo, Y.R., Fishel, M.L., Amundson, S., Kelley, M.R., Smith, M.L., 2002. Implication of p53 in base excision DNA repair: in vivo evidence. Oncogene 21, 731–737.

Smith, M.L., Seo, Y.R., 2002. p53 regulation of DNA excision repair pathways. Mutagenesis 17, 149–156.

Tanaka, T., Suda, T., Suda, J., Inoue, T., Hirabayashi, Y., Hirai, H., Takaku, F., Miura, Y., 1991. Stimulatory effects of granulocyte colony-stimulating factor on colony-forming units-spleen (CFU-S) differentiation and pre-CFU-S proliferation in mice. Blood 77, 2597–2602.

Terracini, B., Testa, M.C., Cabral, J.R., Rossi, L., 1976. The roles of age at treatment and dose in carcinogenesis in C3Hf/Dp mice with a single administration of *N*-nitroso-*N*-methylurea. Br. J. Cancer 33, 427–439.

Till, J.E., McCulloch, E.A., 1961. A direct measurement of the radiation sensitivity of normal mouse bone marrow cells. Radiat. Res. 14, 213–222.

Toft, N.J., Curtis, L.J., Sansom, O.J., Leitch, A.L., Wyllie, A.H., te Riele, H., Arends, M.J., Clarke, A.R., 2002. Heterozygosity for p53 promotes microsatellite instability and tumorigenesis on a Msh2-deficient background. Oncogene 21, 6299–6306.

Tsukada, T., Tomooka, Y., Takai, S., Ueda, Y., Nishikawa, S., Yagi, T., Tokunaga, T., Takeda, N., Suda, Y., Abe, S., Matsuo, I., Ikawa, Y., Aizawa, S-I., 1993. Enhanced proliferative potential in culture of cells from p53-deficient mice. Oncogene 8, 3313–3322.

United Nations Scientific Committee on the Effects of Atomic Radiation 1986. Dose–response relationship for radiation-induced cancer, in: Genetic and Somatic Effects of Ionizing Radiation: United Nations Scientific Committee on the Effects of Atomic Radiation, 1986 Report to the General Assembly, with annexes. United Nations, New York. Annexes B, pp. 1-262.

Weisburger, J.H., Williams, G.M., 1989. Types and amounts of carcinogens as potential human cancer hazards. Cell Biol. Toxicol. 5, 377–391.

Williams, G.M., Iatropoulos, M.J., Jeffrey, A.M., 2000. Mechanistic basis for nonlinearities and thresholds in rat liver carcinogenesis by the DNA-reactive carcinogens 2-acetylaminofluorene and diethylnitrosamine. Toxicol. Pathol. 28, 388–395.

Yamamoto, S., Mitsumori, K., Kodama, Y., Matsunuma, N., Manabe, S., Okamiya, H., Suzuki, H., Fukuda, T., Sakamaki, Y., Sunaga, M., Nomura, G., Hioki, K., Wakana, S., Nomura, T., Hayashi, Y., 1996. Rapid induction of more malignant tumors by various genotoxic carcinogens in transgenic mice harboring a human prototype c-Ha-ras gene than in control non-transgenic mice. Carcinogenesis 17, 2455–2461.

Yoshida, K., Aizawa, S., Watanabe, K., Hirabayashi, Y., Inoue, T., 2002. Stem-cell leukemia: P53 deficiency mediated suppression of leukemic differentiation in C3H/He myeloid leukemia. Leuk. Res. 26, 1085–1092.

Yoshida, K., Inoue, T., Nojima, K., Hirabayashi, Y., Sado, T., 1997. Calorie restriction reduces the incidence of myeloid leukemia induced by a single whole-body radiation in C3H/He mice. Proc. Natl. Acad. Sci. USA 94, 2615–2619.

Yoshida, K., Nemoto, K., Nishimura, M., Hayata, I., Inoue, T., Seki, M., 1986. Nature of leukemic stem cells in murine myelogenous leukemia. Int. J. Cell Cloning 4, 91–102.

Zeise, L., Wilson, R., Crouch, E.A., 1987. Dose–response relationships for carcinogens: a review. Environ. Health Perspect. 73, 259–306.

Targeted disruption of oncostatin M receptor results in altered hematopoiesis

Minoru Tanaka, Yoko Hirabayashi, Takashi Sekiguchi, Tohru Inoue, Motoya Katsuki, and Atsushi Miyajima

Oncostatin M (OSM) is a multifunctional cytokine that belongs to the interleukin 6 (IL-6) family. As OSM is expressed in adult as well as embryonic hematopoietic tissues, OSM has been considered to play a role in hematopoiesis. To uncover roles of OSM, we have generated mutant mice deficient in the OSM-specific receptor β subunit (OSMR). While OSMR$^{-/-}$ mice were healthy and fertile, hematologic analysis of OSMR$^{-/-}$ mice demonstrated that the numbers of peripheral erythrocytes and platelets were reduced compared with wild-type mice. Consistent with this, progenitors of erythroid and megakaryocyte lineages were reduced in OSMR$^{-/-}$ bone marrow (BM), suggesting that OSM is required for the maintenance of erythroid and megakaryocyte progenitor pools in BM. To investigate whether OSM acts on the hematopoietic progenitors directly or indirectly, we performed BM transplantation experiments. The OSMR$^{-/-}$ mice, engrafted with wild-type BM cells, failed to produce erythrocytic and megakaryocytic progenitors to the levels in wild-type mice, indicating that OSM affects hematopoietic microenvironments. On the other hand, erythrocytic and megakaryocytic progenitors were reduced in the wild-type mice reconstituted with OSMR$^{-/-}$ BM cells. Thus, OSM regulates hematopoiesis in vivo by stimulating stromal cells as well as hematopoietic progenitors, in particular megakaryocytic and erythrocytic progenitors. (Blood. 2003;102:3154-3162)

Introduction

Oncostatin M (OSM) is a multifunctional cytokine and is a member of the interleukin 6 (IL-6) family that includes IL-6, IL-11, leukemia inhibitory factor (LIF), ciliary neurotrophic factor (CNTF), cardiotrophin-1, and novel neutrophin-1/B-cell–stimulating factor-3.[1-3] Among the family members, OSM is the most closely related to LIF structurally, genetically, and functionally.[4,5] OSM was initially recognized by its biologic activity to inhibit the proliferation of A375 melanoma cells and its cDNA was originally isolated from phorbol ester–stimulated human histiocytic lymphoma U937 cells.[6] It is known that OSM is secreted from activated T cells and monocytes stimulated by cytokines and plays roles in inflammatory reactions.[7,8] In humans, OSM and LIF exhibit various overlapping biologic responses such as growth regulation, differentiation, gene expression, and cell survival, while it is also known that OSM displays some unique biologic properties that are not shared with LIF (eg, growth inhibition of A375 melanoma cells,[9] growth of AIDS-related Kaposi sarcoma cells in an autocrine manner,[10] and up-regulation of α1-proteinase inhibitor in lung-derived epithelial cells).[11] These common and unique functions of OSM are now well explained by the receptor structures. Two types of functional OSM receptors are present in humans; the type I OSM receptor is identical to the high-affinity LIF receptor that consists of gp130 and the LIF receptor β subunit[12,13] and the type II OSM receptor consists of gp130 and the OSM-specific receptor β subunit (OSMR).[14,15] Thus, many overlapping biologic responses between human OSM (hOSM) and hLIF are mediated by the shared type I receptor (ie, the LIF receptor), whereas OSM manifests its specific responses through the type II receptor. OSMR is expressed in a wide variety of cell types including endothelial cells, hepatic cells, lung cells, skin cells, and many tumor cell lines.[16-20] Curiously, unlike hOSM, mouse OSM (mOSM) transduces its signals through the OSM-specific receptor consisting of gp130 and OSMR but does not use the type I OSM receptor (ie, the LIF receptor).[21]

Previously we isolated mOSM cDNA as a signal transducer and activator of transcription 5 (Stat5)–inducible gene in hematopoietic cells by the cDNA subtraction method and found that mOSM is expressed in hematopoietic tissues such as bone marrow (BM) and spleen, suggesting that mOSM may play a role in hematopoiesis.[22] OSM is expressed not only in adult tissues but also in embryonic hematopoietic tissues. We found that mOSM is expressed in the embryonic aorta-gonad-mesonephros (AGM) region where definitive hematopoiesis originates and that mOSM stimulates generation of hematopoietic cells and endothelial cells in the primary culture of the AGM cells, possibly acting on their common precursors.[23] Moreover, mOSM is also expressed in CD45^{+} hematopoietic cells in fetal liver and stimulates differentiation of fetal hepatocytes, suggesting that OSM may coordinate development of hematopoiesis and liver.[24,25] In adults, while there are many reports that OSM functions as a proinflammatory factor, the role of OSM in steady-state hematopoiesis in vivo remains largely unknown. In this report, we describe the generation of OSMR-deficient mice and the role of OSM in hematopoiesis in vivo.

From the Institute of Molecular and Cellular Biosciences, University of Tokyo, Japan; Kanagawa Academy of Science and Technology, Kawasaki, Japan; National Institute of Health Sciences, Tokyo, Japan; and National Institute for Basic Biology, Okazaki National Research Institute, Okazaki, Japan.

Submitted February 4, 2003; accepted June 28, 2003. Prepublished online as *Blood* First Edition Paper, July 10, 2003; DOI 10.1182/blood-2003-02-0367.

Supported in part by Grants-in-Aid for Scientific Research and Special Coordination Funds from the Ministry of Education, Culture, Sports, Science and Technology of Japan; a research grant from the Ministry of Health, Labour and Welfare, and Core Research for Evolutional Science and Technology (CREST) of the Japan Science and Technology Corporation.

Reprints: Minoru Tanaka, Institute of Molecular and Cellular Biosciences, University of Tokyo, 1-1-1 Yayoi, Bunkyo-ku, Tokyo 113-0032, Japan; e-mail: tanaka@iam.u-tokyo.ac.jp.

The publication costs of this article were defrayed in part by page charge payment. Therefore, and solely to indicate this fact, this article is hereby marked "advertisement" in accordance with 18 U.S.C. section 1734.

Materials and methods

Mice

C57/BL6 mice (8-12 weeks) were purchased from Japan SLC (Hamamatsu, Japan). Green fluorescent protein (GFP) mice were from Dr M. Okabe (Keio University, Tokyo, Japan).[26]

Targeted disruption of OSMR by homologous recombination in embryonic stem cells

The targeting vector was constructed by inserting the LacZ-neomycin phosphotransferase (pgkNeo) cassette for positive selection (a kind gift of Dr Takahashi, Tsukuba University, Tsukuba, Japan) and the MC1–diphtheria toxin (DT-A) cassette for negative selection. The *Apa*I site was introduced at the 18-bp downstream from ATG to fuse LacZ to ATG in frame. The 5′ 1.8-kb *Hin*dIII-*Apa*I fragment and the 3′ 7.2-kb *Sac*II-*Bgl*II fragment were inserted upstream and downstream of the LacZ-pgkNeo cassette, respectively. The DT-A cassette was inserted at the 5′ side. The construct was linearized by *Bgl*II and electroporated into CCE embryonic stem (ES) cells. G418-resistant ES cell clones were isolated, expanded, and screened by Southern blot analysis. Genomic DNA was digested with *Eco*RV, transferred onto a nylon membrane, and prehybridized and hybridized at 45°C in high-sodium dodecyl sulfate (SDS) buffer (Roche Diagnostics, Mannheim, Germany) and probed with a 700-bp *Eco*RI-*Bgl*II fragment (5′ probe) derived from the cloned genomic DNA fragment. The labeling of probe and detection were performed using the Digoxigenin (DIG) system (Roche Diagnostics) according to the manufacturer's protocol. Predicted size of the wild-type DNA fragment detected by 5′ probe is 9.0 kb and that of the mutant DNA is 6.5 kb. These cells were injected into blastocysts. The chimeric mice were mated with C57/BL6 female mice and the heterozygous offspring were interbred to yield wild-type, heterozygous, and mutant mice. Genotyping was performed by polymerase chain reaction (PCR) using specific primers from genomic DNA derived from their tails. PCR reactions were performed in 50 μL with 1 × PCR buffer (Takara, Tokyo, Japan), 0.2 mM each of dNTP (deoxynucleoside triphosphate), 0.5 U Taq polymerase (Takara), and 10 pmol of each primer: 5′-GTAATCAGACCAATGGCTTTCTC-3′, 5′-GATCCAACAGAGCAATCATGAAGC-3′, and 5′-GCACATCTGAACTTCAGC-3′. Amplification conditions were an initial denaturation at 94°C for 2 minutes followed by 35 cycles of 94°C for 1 minute, 60°C for 1 minute, and 72°C for 90 seconds. The wild-type mice generated a 364-bp PCR product, whereas the $OSMR^{-/-}$ mice had only a 750-bp fragment. The heterozygous mice had both fragments.

Northern blot analysis

Lung mRNA was prepared from adult lung derived from wild-type, heterozygous, and mutant mice with the FastTrack mRNA purification kit (Invitrogen, Carlsbad, CA). Standard Northern blot analysis of 1 μg mRNA was performed. A 502-bp fragment (nucleotides 1166-1667 from GenBank accession no. AB015978) was DIG-labeled by PCR using primers (5′-CAACTGGAGTTCCTGGAAAG-3′ and 5′-AGTGATTTGCCAGGTATAGG-3′) and DIG DNA labeling Mix (Roche Diagnostics) and then used for Northern blotting.

Hematologic analysis

Orbital plexus blood was collected from anesthetized mice. Peripheral blood cells were analyzed by using an automated counter Sysmex K-4500 (TOA Medical Instruments, Kobe, Japan). BM and spleen progenitor cells were assayed using semisolid methylcellulose cultures as previously described.[27] In short, 25 000 BM or 100 000 spleen nucleated cells were plated in triplicate in 1-mL methylcellulose culture. Cells were cultured in the presence of combinations of purified recombinant growth factors at the following final concentrations: murine erythropoietin (EPO; Roche Diagnostics) at 4 U/mL, human stem cell factor (SCF; Sigma Chemical, St Louis, MO) at 80 ng/mL, murine IL-3 at 10 ng/mL. After 3 days of incubation in a fully humidified atmosphere at 37°C supplemented with 5% CO_2, erythroid colony-forming units (CFU-Es) were counted. Granulocyte-macrophage colony-forming cells (GM-CFCs), erythroid burst-forming units (BFU-Es), granulocyte-erythrocyte-megakaryocyte-macrophage CFUs (CFU-GEMMs), and megakaryocyte-erythrocyte CFUs (CFU-MEs) were enumerated after 7 days of incubation. Average counts of triplicate cultures are presented in each experiment. Megakaryocytic progenitors were assessed by liquid culture of BM. Nucleated BM cells (100 000 cells) were incubated in Iscove modified Dulbecco medium (IMDM) containing 1% Nutridoma SP (Roche Diagnostics) and thrombopoietin (TPO; Sigma Chemical) at 25 ng/mL in a 96-well plate at 37°C supplemented with 5% CO_2 for 3 days. Mature megakaryocyte was identified by acetylcholinesterase (AchE) staining.[28] Plates were fixed with 2.5% glutaraldehyde at room temperature for 20 minutes. After washing with phosphate-buffered saline (PBS; twice), AchE staining solution (0.5 mg acetylthiocholine iodide in 1 mL of 5 mM sodium citrate, 1.5 mM $CuSO_4$, 0.25 mM potassium ferricyanide) was added into the plate. After 1 hour of incubation at 37°C, AchE-positive cells were counted.

Phenylhydrazine and 5-FU administration

A single dose of phenylhydrazine (60 mg/kg body weight) was administered intraperitoneally for 2 consecutive days. Wild-type and mutant mice were killed at 1, 2, 4, and 7 days after the final administration. CFU-Es of 25 000 BM nucleated cells were assessed by semisolid methylcellulose cultures as described in hematologic analysis. Likewise, a single dose of 5-fluorouracil (FU; 150 mg/kg body weight) was administered intravenously. Wild-type and mutant mice were killed at 2, 5, and 8 days after administration. Then, 50 000 (days 2) and 25 000 (days 5 and 8) BM nucleated cells were assessed by semisolid methylcellulose cultures as described in hematologic analysis.

Flow cytometry

Marrow cells were flushed from the femurs with a syringe containing 2 mL alfa-MEM-10% FCS (α-modified minimum essential media–10% fetal calf serum). After depletion of mature red cells by hypotonic lysis (0.38% NH_4Cl for 7 minutes on ice), the GPF-positive cells were sorted from mononuclear cells of BM and spleen by FACS Vantage (Becton Dickinson Labware, Bedford, MA) and used for semisolid methylcellulose cultures.

Transplantation assay

Transplantation of cells into busulfan-treated neonatal mice was performed as previously described[29] with a slight modification. In short, pregnant recipient mice were intraperitoneally injected with busulfan (Sigma Chemical) at 12.5 mg/kg body weight on pregnancy days 17 and 18. The transplanted cells were prepared from BM of a GPF-expressing wild-type or mutant mouse followed by negative selection for lineage markers such as TER119, Gr-1, CD4, and CD8 (PharMingen, San Diego, CA). Then, 24 to 48 hours after birth, 7×10^5 cells in 25 μL of PBS were injected into each neonatal liver. To measure the chimerism of GFP-positive cells in recipient mice, orbital plexus blood was collected from anesthetized mice to a heparinized capillary tube and centrifuged at 800*g* for 10 minutes. The white blood cell layer at the interface was collected into PBS, then mature red cells were depleted by hypotonic lysis. The chimerism of GFP-positive cells was measured by fluorescence-activated cell sorter (FACS) analysis of white blood cells.

RT-PCR

Total RNA was prepared from wild-type and mutant BM and spleen by TRIzol reagent (Gibco BRL, Grand Island, NY) according to the manufacturer's instruction. For reverse transcriptase–PCR (RT-PCR) analysis, first-strand cDNA was synthesized from total RNA by the First-Strand cDNA Synthesis Kit (Amersham Biosciences, Piscataway, NJ). Each sample was prepared from 3 mice of the same genotype. Synthesized cDNA samples were used as templates for PCR amplification for OSM, SCF, and GAPDH (glyceraldehyde phosphate dehydrogenase). Amplification conditions were as follows: an initial denaturation at 96°C for 30 seconds

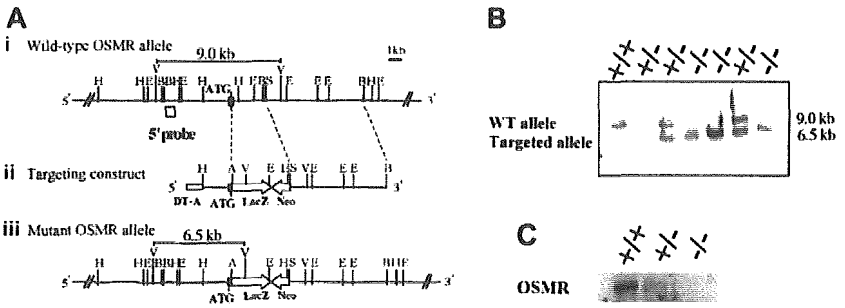

Figure 1. Targeting disruption of the mOSMR gene. (Panel A) Targeting strategy of the mOSMR gene. (i) Schematic diagram of the wild-type allele. The start codon is indicated by ATG. The open box represents the location of the probe used to detect the restriction fragment of genomic DNA by Southern blot analysis. Restriction enzyme sites are indicated as *ApaI* (A), *EcoRI* (E), *EcoRV* (V), *HindIII* (H), *BglII* (B), and *SacII* (S). (ii) Gene targeting vector. The vector contains the 5′ and 3′ regions of homology and the cDNAs encoding neomycin transferase (Neo), LacZ, and diphtheria toxin (DT-A). (iii) Diagram of the targeted mutant OSMR allele. (Panel B) Southern blot analysis of the *EcoRV*-digested genomic DNA extracted from the $OSMR^{+/+}$, $OSMR^{+/-}$, and $OSMR^{-/-}$ mice. (Panel C) Northern blot analysis of neonatal lung mRNA ($^{+/+}$, $^{-/-}$, and $^{-/-}$) with mOSMR probe.

followed by 28 to 44 cycles of 96°C for 20 seconds, 52°C for 30 seconds, and 72°C for 90 seconds. PCR primers used in this study were as follows: OSM (5′-CATCCTGAGCATGGCACTGG-3′ and 5′-GCCACAGCTGC-CTATCTTGG-3′), SCF (5′-TCTTCCAAATGACTATATGATAACCCTC-3′ and 5′-ATTCCTAAGGGAGCTGGCTGCAACAGGG-3′), and GAPDH as a positive control (5′-ACCACAGTCCATGCCATCAC-3′ and 5′-TCCACCACCCTGTTGCTGTA-3′).

Results

Generation of OSMR-deficient mice

In order to disrupt the OSMR gene, the proximal region of the initiation codon was replaced with the LacZ and neomycin expression cassette, resulting in the deletion of the N-terminal region including the signal sequence (Figure 1A). Neomycin-resistant ES cells were screened by Southern blot using a probe corresponding to the 5′ end of the targeting construct. One of 6 successfully targeted ES clones heterozygous for the OSMR locus was injected into blastocysts to generate chimeric mice. Intercross of heterozygous mice resulted in 3 genotypes of mice (wild-type $OSMR^{+/+}$, heterozygous $OSMR^{+/-}$, and homozygous $OSMR^{-/-}$; Figure 1B), and they were born with a normal mendelian pattern of inheritance. The growth rate of $OSMR^{-/-}$ mice was comparable to wild-type littermates from neonate to adult. These results indicate that $OSMR^{-/-}$ mice have no apparent growth disadvantage. To confirm the disruption of the OSMR locus, we performed Northern blot analysis using RNA prepared from the lung with an OSMR cDNA probe, as it is known that OSMR was highly expressed in lung.[30] A single band corresponding to mOSMR mRNA was detected in wild-type and heterozygous mRNA, whereas no such signal was present in homozygous mice (Figure 1C). To further verify the elimination of OSMR function by targeting, we used 2 primary culture systems using fetal liver and the AGM region, which were previously shown to respond to mOSM.[23,24] Neither of the culture systems derived from $OSMR^{-/-}$ mice responded to OSM (data not shown), indicating the lack of functional OSMR in the homozygous mice.

OSM was previously shown to stimulate Sertoli cells in vitro, suggesting a role for OSM in reproduction.[31] However, as OSMR null mice bred normally, these mice were intercrossed with C57/BL6 repeatedly for at least 8 generations and used for further analysis.

Hematologic analysis

Since OSM is expressed in hematopoietic tissues, we first analyzed the peripheral blood cells in $OSMR^{-/-}$ mice. The number of white blood cells in the peripheral blood was comparable among genotypes (data not shown). In contrast, the red cell number in the peripheral blood of the $OSMR^{-/-}$ mice was reduced compared with the wild-type mice ($894 \pm 64 \times 10^4$/mL in $OSMR^{-/-}$ vs $987 \pm 52 \times 10^4$/mL in $OSMR^{+/-}$ vs $1028 \pm 52 \times 10^4$/mL in $OSMR^{+/+}$ mice; Figure 2A). Consistent with this reduction, the hematocrit of $OSMR^{-/-}$ mice was also reduced. Interestingly, the platelet number in the peripheral blood of $OSMR^{-/-}$ mice was also reduced ($82 \pm 10 \times 10^4$/mL in $OSMR^{-/-}$ vs $78 \pm 13 \times 10^4$/mL in $OSMR^{+/-}$ vs $106 \pm 15 \times 10^4$/mL in $OSMR^{+/+}$ mice; Figure 2B). Although there are reports describing effects of the IL-6–family cytokines such as IL-6, IL-11, and LIF on proliferation and differentiation of megakaryocytes in vitro[32-34] and in vivo,[35-37] no mice with mutant alleles of either cytokine or its specific receptor have been reported to show thrombocytopenia.[38-40] Therefore, mOSM may be the most important IL-6–family cytokine for megakaryopoiesis in vivo.

Since OSM is highly expressed in BM,[22] we hypothesized that OSM would affect the maintenance of hematopoietic progenitors in BM. To examine this possibility, we counted the number of hematopoietic progenitors in BM by in vitro clonal cultures with multiple cytokine combinations. The number of CFU-Es, the proerythroblasts, was significantly reduced in $OSMR^{-/-}$ BM compared with the wild-type control (Figure 3A). The number of erythrocyte-producing colonies (ie, CFU-GEMMs, CFU-MEs, and BFU-Es) was also significantly reduced in $OSMR^{-/-}$ BM

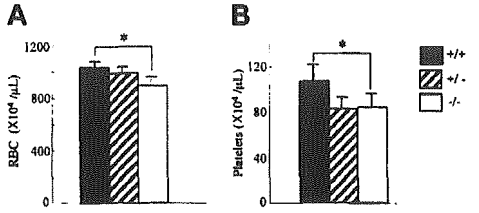

Figure 2. Hematologic profiles of $OSMR^{+/+}$, $OSMR^{+/-}$, and $OSMR^{-/-}$ mice. Orbital plexus blood was collected from anesthetized mice. Peripheral red blood cells (RBCs; panel A) and platelets (B) were analyzed by using automated counter Sysmex K-4500. Numbers show mean cell number ± SD ($n = 17$ of $OSMR^{+/+}$ and $OSMR^{+/-}$, $n = 6$ of $OSMR^{-/-}$ for RBCs; $n = 14$ of $OSMR^{+/+}$ and $OSMR^{+/-}$, $n = 6$ of $OSMR^{-/-}$ for platelets). *$P < .001$ between wild-type and mutant mice.